SUPPORTING INFORMATION

for

Preparation of Different Conjugated Polymers Characterized by Complementary Electronic Properties from an Identical Precursor

Marco Carlotti, Tommaso Losi, Francesco De Boni, Federico Maria Vivaldi, Esteban Araya-Hermosilla, Mirko Prato, Andrea Pucci, Mario Caironi, Virgilio Mattoli

INDEX

Materials and Methods

Triisopropylsilylacetylene, trimethylsilylchloride, methyl iodide, phenylacetylene, bis(dibenzylideneacetone) palladium(0), tri(o-toluyl)phosphine, 5,5'-bis(trimethylstannyl)-2,2'-bithiophene, methyl lithium 1.6 M in diethyl ether, acetic acid, hydrochloric acid 37%, methylisobutylketone, o-dichlorobenzene and tin(II) chloride were purchased from Merck Life Sciences (Italy). 2,6-dibromoanthraquinone, 1-octyne, 4-tertbutyl-1-bromobenzene, tetrabutylammoniumfluoride 1 M in THF were purchased from TCI Europe (Belgium). Parylene N was obtained from Specialty Coating Systems (IN, USA). Anhydrous solvents employed in the reactions were obtained from a house system.

IR-ATR spectra were recorded on a Shimadzu IRAffinit-1 spectrometer mounting a MIRacle 10 ATR module. IR maps were recorded on a Thermo Scientific Nicolet iN10 MX employing transmission mode a BaF_2 substrate.

NMR (^1H and proton-decoupled ^{13}C) characterization of the compounds was performed on a Bruker Avance DRX 400 spectrometer at room temperature and employing the chloroform residual peak as internal standard. The spectra were analyzed employing Mestrenova (v14.1.2).

The elemental composition of the polymers was determined via an Elementar Vario Micro Cube for sulfur, nitrogen, carbon and hydrogen.

Thermogravimetric analysis (TGA) was performed on a Mettler Toledo TGA/SDTA851 instrument under nitrogen flux (80 mL/min).

Gel Permeation Chromatography (GPC) measurements were performed with an HP1100 Hewlett-Packard employing polymer solutions in chloroform with a maximum concentration of 0.5 mg/mL previously filtered through a Teflon filter with 0.22 µm pore size and employing PS as standard.

UV-Vis spectroscopy was performed on an Agilent Cary 5000 UV–vis–NIR spectrophotometer.

Fluorescence spectra were acquired on a Horiba Jobin–Yvon Fluorolog-3 spectrofluorometer equipped with a 450 W xenon arc lamp, double-grating excitation, and single-grating emission monochromator.

Cyclic Voltammetry (CV) experiments were performed in a conventional three electrodes electrochemical cell using a Palmsens EmStatS4 (Palmsens, The Netherland) employing a Pt wire as counter electrode and as reference an Ag wire immersed in a 0.1 M $AgNO_3$ solution in acetonitrile in contact with the solution through a porous septum (IS-AG.NA.RE, ItalSens; V vs SHE = 0.36 V); the measurements of the thin films on either evaporated Au or ITO were performed in acetonitrile employing tetrabutyl-ammonium hexafluorophosphate (Bu_4NPF_6) 0.1 M as electrolyte. Local conductivity experiments were performed using a MultiEmStat (Palmsens, The Netherlands) in floating mode. Pt and silver wires were used as counter and reference electrode, respectively. An interdigitated gold electrode was used as working electrode applying a bias of 20 mV between the two gold branches. CV experiments at 50 mV/s using the experimental conditions previously reported. The conductive current was then obtained knowing that the total current for each electrode could be expressed as:[1]

$$i_1 = i_{f1} + i_{\Omega} \quad (1)$$

$$i_2 = i_{f2} - i_{\Omega} \quad (2)$$

Where i_f is the faradaic current and i_{Ω} is the ohmic current.

Atomic Force Microscopy (AFM) and solid-state (ss) NMR ^{13}C measurements were performed through the CISUP facilities of the University of Pisa. In particular, AFM topography, phase, and error images were acquired using a Multimode microscope equipped with a Nanoscope IV controller (Veeco, now Bruker). Images were recorded in tapping mode employing a RTESP tip (tip height: 15 µm – 20 µm; front angle: 15°; back angle: 25°; side angle: 17.5°; tip radius nom.: <10 nm; tip radius max.: 12.5 nm) and analyzed employing Gwyddion (v2.57). During the scan, the amplitude was reduced by 25% from its free value. ssNMR spectra were acquired on a Bruker Avance Neo spectrometer (Bruker Italia S.r.l., Italy) working at the Larmor frequency of 500.13 MHz and 125.77 MHz for ^1H and ^{13}C, respectively, equipped with a 4 mm CP-MAS probe head. All measurements were performed at 25 °C at a MAS frequency of 15 kHz. ^1H-^{13}C CP-MAS spectra were performed using a contact time of 5 ms, a relaxation delay of 5 s; High-Power Decoupling (HPD) from ^1H nuclei was applied during acquisition. 3200-3600 scans were accumulated for all ^1H-^{13}C CP-MAS spectra. For

all experiments, a π/2 pulse of 3.85 and 3.90 µs was used for ^{1}H and ^{13}C, respectively. ^{13}C chemical shifts were referred to adamantane and TMS as secondary and primary references, respectively.

Parylene N was deposited employing a Parylene Coater PDS2010 (Specialty Coating Systems, IN, USA) following the parameters suggested by the manufacturer.

Scanning electron microscopy (SEM) images of the nanofilm on PEN were obtained with a Dual Beam FIB/SEM Helios Nano-Lab 600i (FEI, The Netherlands) employing the parameters reported in the bottom part of the pictures.

X-ray photoelectron spectroscopy (XPS) measurements were carried out through a Kratos Axis Ultra^{DLD} spectrometer (Kratos Analytical Ltd.) with monochromated Al K_α X-ray source (*hv* = 1486.6 eV) operating at 20 mA and 15 kV. The samples, composed of a thin film of the polymer over an indium-tin-oxide (ITO) substrate, were mounted on the sample holder *via* copper tape to maximize its electrical conductivity.
The wide scans were collected over an analysis area of 300 × 700 µm^2 at a photoelectron pass energy of 160 eV and energy step of 1 eV. Differential electrical charging effects on the surface of the sample were neutralized during the measurements of all specimens. The spectra were analyzed with the CasaXPS software (Casa Software Ltd., version 2.3.24).

The ultraviolet (UPS) photoelectron spectroscopy measurements were performed using a He I (21.22 eV) discharge lamp, fitted in the same chamber used for XPS analyses, on an area of 55 µm in diameter, at a pass energy of 10 eV and with a dwell time of 100 ms. Spin-coated films of the different polymers were used for this analysis. The position of the HOMO level versus the vacuum level, i.e., the ionization energy, was determined for each sample by measuring the width of the entire UPS spectrum, from the secondary edge cutoff to the position of the HOMO level itself[2] (see Figure SI14). These positions were determined in the UPS spectrum through the background functions “Edge Up” and “Edge Down”, respectively, in the CasaXPS software (Casa Software Ltd., version 2.3.24). The error bar associated with this procedure was estimated equal to 0.2 eV.

Synthesis of the precursors

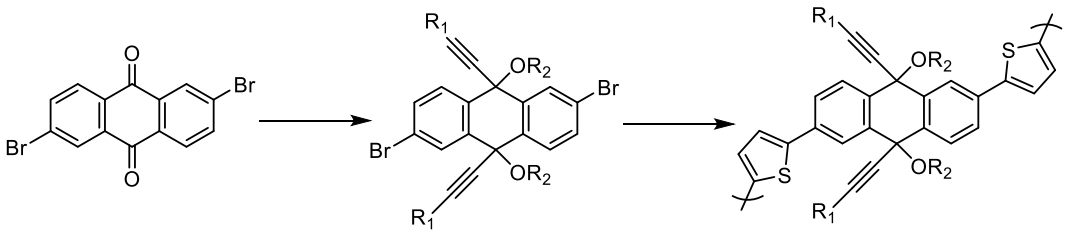

1: R_1= TIPS, R_2= TMS
2: R_1= TIPS, R_2= Me
3: R_1= Ph, R_2= TMS
4: R_1= C_6H_{13}, R_2= TMS

AH-P: R_1= TIPS, R_2= TMS
2-P: R_1= TIPS, R_2= Me
3-P: R_1= Ph, R_2= TMS
4-P: R_1= C_6H_{13}, R_2= TMS

Synthesis of ((2,6-dibromo-9,10-bis((trimethylsilyl)oxy)-9,10-dihydroanthracene-9,10-diyl)bis(ethyne-2,1-diyl))bis(triisopropylsilane), ***1***

In a dry 100 mL flask under nitrogen, 1.6 mL of triisopropylsilyacetylene (TIPS-acetylene; 6.9 mmol, 2.55 Eq) were dissolved in 50 mL of dry tetrahydrofuran (THF) and the solution placed in an ice bath. 4.6 mL of methyllithium 1.6 M in diethyl ether (6.8 mmol, 2.5 Eq) were added dropwise and the reaction left for 20 minutes. 1 g of 2,6-dibromoanthraquinone (2.7 mmol, 1 Eq) was added and the bath removed. After 1

hour, 2 mL of trimethylsilyl chloride (TMSCl) was added. The solution was then extracted with a saturated aqueous ammonium chloride solution and dried over magnesium sulfate. The solvent was removed under vacuum, and the residue recrystallized twice from ethyl acetate to obtain 1.05 g of product as white crystals (45% yield). Alternatively, the purification can be performed through column chromatography (SiO_2, hexane:ethylacetate 10:1, Rf= 0.8). ^{1}H NMR (400 MHz, Chloroform-d) δ (ppm):8.09 (d, J = 2.1 Hz, 1H), 7.80 (d, J = 8.5 Hz, 1H), 7.53 (dd, J = 8.5, 2.1 Hz, 1H), 1.05 (s, 21H), -0.28 (s, 9H). ^{13}C NMR (101 MHz, Chloroform-d) δ (ppm): 138.67, 135.45, 132.29, 131.90, 131.05, 122.56, 111.16, 87.24, 67.97, 18.63, 11.32, 1.42. Elem. Anal. $C_{42}H_{66}Br_2O_2Si_4$ Calc. (%) C 57.64 H 7.60 Br 18.26 O 3.66 Si 12.84. Exp. (%) C 57.54 H 7.622.

Synthesis of ((2,6-dibromo-9,10-bis((trimethoxy)-9,10-dihydroanthracene-9,10-diyl)bis(ethyne-2,1-diyl))bis(triisopropylsilane), ***2***

A similar procedure for the synthesis of **1** was followed, employing 3 mL of iodomethane in place of TMSCl and let the reaction under stirring overnight (53% yield). ^{1}H NMR (400 MHz, Chloroform-d) δ (ppm): 8.14 (d, J = 2.1 Hz, 1H), 7.82 (d, J = 8.5 Hz, 1H), 7.61 (dd, J = 8.5, 2.1 Hz, 1H), 2.80 (s, 3H), 1.03 (d, J = 2.8 Hz, 19H). ^{13}C NMR (101 MHz, Chloroform-d) δ (ppm): 137.82, 134.40, 132.40, 131.26, 130.00, 123.33, 108.01, 89.39, 72.03, 51.33, 18.61, 11.18. Elem. Anal. $C_{38}H_{54}Br_2O_2Si_2$ Calc. (%) C 60.15 H 7.17 Br 21.06 O 4.22 Si 7.40. Exp. (%) C 60.10 H 7.291

Synthesis of ((2,6-dibromo-9,10-bis((trimethylsilyl)oxy)-9,10-dihydroanthracene-9,10-diyl)bis(ethyne-2,1-diyl))bis(phenylene), ***3***

A similar procedure for the synthesis of **1** was followed, employing phenylacetylene in place of TIPS-acetylene (44% yield). ^{1}H NMR (400 MHz, Chloroform-d) δ (ppm): 8.13 (d, *J* = 2.1 Hz, 1H), 7.88 (d, *J* = 8.4 Hz, 1H), 7.56 (dd, *J* = 8.5, 2.1 Hz, 1H), 7.43 – 7.36 (m, 2H), 7.30 (m, 3H), -0.06 (s, 9H). ^{13}C NMR (101 MHz, $CDCl_3$) δ (ppm): 139.76, 136.73, 131.87, 131.63, 131.04, 129.97, 128.70, 128.30, 122.70, 122.34, 92.11, 87.07, 77.33, 77.01, 76.70, 68.93, 1.64. Elem. Anal. $C_{36}H_{34}Br_2O_2Si_2$ Calc. (%) C 60.51 H 4.80 Br 22.36 O 4.48 Si 7.86. Exp. (%) C 60.22 H 4.596

Synthesis of ((2,6-dibromo-9,10-bis((trimethylsilyl)oxy)-9,10-dihydroanthracene-9,10-diyl)bis(oct-1-yne), ***4***

A similar procedure for the synthesis of **1** was followed, employing 1-octyne in place of TIPS-acetylene (22% yield). ^{1}H NMR (400 MHz, Chloroform-d) δ (ppm): 8.05 (d, J = 2.1 Hz, 1H), 7.79 (d, J = 8.5 Hz, 1H), 7.52 (dd, J = 8.4, 2.1 Hz, 1H), 2.24 (t, J = 7.1 Hz, 2H), 1.56 – 1.42 (m, 2H), 1.39 – 1.18 (m, 2H), 0.88 (t, J = 6.8 Hz, 3H), -0.11 (s, 9H). ^{13}C NMR (101 MHz, Chloroform-d) δ (ppm): 139.87, 136.80, 131.58, 131.19, 130.15, 122.38, 88.16, 83.87, 68.45, 31.35, 28.66, 22.61, 19.08, 14.12, 1.63. Elem. Anal. $C_{36}H_{50}Br_2O_2Si_2$ Calc. (%) C 59.17 H 6.90 Br 21.87 O 4.38 Si 7.69. Exp. (%) C 59.46 H 7.027

Stille polymerization of ((2,6-dibromo-9,10-bis((triisopropylsilyl)ethynyl)-9,10-dihydroanthracene-9,10-diyl)bis(oxy))bis(trimethylsilane) and 5,5'-bis(trimethylstannyl)-2,2'-bithiophene, ***AH-P***

In a dry 50 mL Schenk under argon, 300 mg of **1** (0.34 mmol, 1 Eq) and 177 mg of 5,5'-bis(trimethylstannyl)-2,2'-bithiophene (0.34 mmol) were dissolved in 22 mL of dry toluene and the solution degassed. 17 mg of bis(dibenzylideneacetone)palladium(0) (0.03 mmol, 0.1 Eq) and 37 mg of tri(o-toluyl)phosphine (0.12 mmol, 0.4 Eq) were added and the reaction left at 110 °C for 4 hours. 0.2 mL of 4-tertbutyl-1-bromobenzene were added and the reaction left for one additional hour. The solution was then poured in

250 mL of methanol and the precipitate extracted with hot acetone and hot chloroform. The chloroform fraction was precipitated in methanol to obtain a yellow-green powder (156 mg, 77% yield). ^{1}H NMR (400 MHz, Chloroform-d) δ (ppm): 8.26 (s, 1H), 8.01 (d, J = 8.2 Hz, 1H), 7.71 (d, J = 8.4 Hz, 1H), 7.41 (d, J = 3.7 Hz, 1H), 7.27 (s, 1H), 1.10 (s, 21H), -0.22 (s, 9H). ^{13}C NMR (101 MHz, Chloroform-d) δ (ppm): 142.69, 137.49, 136.98, 136.09, 134.02, 129.98, 126.06, 125.57, 124.06, 111.96, 86.43, 68.40, 18.69, 11.37, 1.51. NMR spectra asre shown in Figures Si1 and SI6. Elem. Anal. $C_{50}H_{70}O_2S_2Si_4$ Calc. (%) C 68.28 H 8.02 O 3.64 S 7.29 Si 12.77. Exp. (%) C 67.21 H 7.784 S 7.352. Mn= 12383 Da, Mw= 44407 Da, PDI= 3.58.

*Stille polymerization of **2** and 5,5'-bis(trimethylstannyl)-2,2'-bithiophene, **2-P***

A similar procedure for the synthesis of **AH-P** was followed. The polymer was obtained as an orange powder (85% yield). ^{1}H NMR (400 MHz, Chloroform-d) δ (ppm): 8.28 (s, 1H), 8.04 (d, J = 8.0 Hz, 1H), 7.77 (d, J = 8.1 Hz, 1H), 7.43 (s, 1H), 7.28 (s, 1H) 2.88 (s, 3H), 1.09 (s, 21H). Mn= 18211 Da, Mw= 34656 Da, PDI= 1.90.

*Stille polymerization of **3** and 5,5'-bis(trimethylstannyl)-2,2'-bithiophene, **3-P***

A similar procedure for the synthesis of **AH-P** was followed. The polymer was obtained as an orange powder (83% yield). ^{1}H NMR (400 MHz, $CDCl_3$) δ (ppm): 8.34 (s, 1H), 8.12 (d, *J* = 7.7 Hz, 1H), 7.76 (d, *J* = 8.3 Hz, 1H), 7.55 – 7.45 (m, 2H), 7.42 (s, 1H), 7.38 – 7.31 (m, 3H), 0.04 (d, *J* = 2.1 Hz, 9H). ^{13}C NMR (101 MHz, Chloroform-d) δ (ppm): 142.80, 138.58, 137.23, 137.06, 134.23, 129.01, 128.49, 125.71, 125.19, 124.84, 124.28, 122.75, 93.09, 86.72, 69.39, 1.79. Mn= 17164 Da, Mw= 65721 Da, PDI= 3.83.

*Stille polymerization of **4** and 5,5'-bis(trimethylstannyl)-2,2'-bithiophene, **4-P***

A similar procedure for the synthesis of **AH-P** was followed. The polymer was obtained as a yellow powder (73% yield). ^{1}H NMR (400 MHz, Chloroform-d) δ (ppm): 8.28 (s, 1H), 8.04 (d, J = 8.0 Hz, 1H), 7.77 (d, J = 8.1 Hz, 1H), 7.43 (s, 1H), 7.28 (s, 1H) 2.88 (s, 3H), 1.09 (s, 21H). ^{13}C NMR (101 MHz, Chloroform-d) δ (ppm): 142.93, 138.60, 137.31, 136.93, 133.85, 129.09, 128.48, 125.39, 124.70, 124.06, 123.56, 87.56, 84.66, 68.82, 31.34, 28.65, 28.37, 22.53, 19.13, 14.03, 1.71. Mn= 34837 Da, Mw= 134986 Da, PDI= 3.87.

*Stille polymerization of 2,6-dibromoanthraquinone and 5,5'-bis(trimethylstannyl)-2,2'-bithiophene, **AQ-DP***

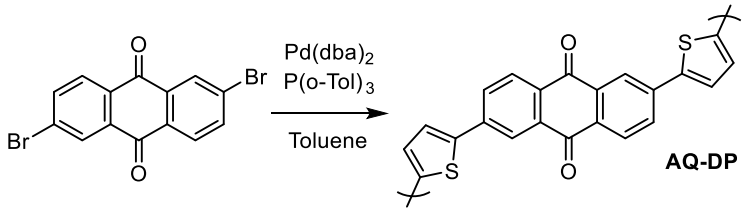

A similar procedure for the polymerization of **AH-P** reported above was followed. In a dry 50 mL Schenk under argon, 100 mg of dibromoanthraquinone (0.27 mmol, 1 Eq) and 141 mg of 5,5'-bis(trimethylstannyl)-2,2'-bithiophene (0.29 mmol, 1.05 Eq) were dissolved in 20 mL of dry toluene and the solution degassed. 16 mg of bis(dibenzylideneacetone)palladium(0) (0.03, 0.1 Eq) and 34 mg of tri(o-toluyl)phosphine (0.12 mmol, 0.4 Eq) were added and the reaction left at 110 °C for 1.5 hour. Longer reaction times resulted in the formation of a large fraction of intractable solid. The solution was pale orange fluorescent. After 1 hour, the fluorescence was not noticeable anymore. 0.2 mL of 4-tertbutyl-1-bromobenzene were added and the reaction left for one additional hour. The solution was then poured in 200 mL of methanol and the precipitate

extracted with hot acetone and hot chloroform. The chloroform fraction was precipitated in methanol to obtain a red powder (8 mg, 13% yield). The IR spectrum shown in Figure 1 was taken on the non-soluble fraction after washing with boiling acetone and chloroform. Mn= 511 Da, Mw= 734 Da, PDI= 1.44.

Synthesis of ((2,6-dibromoanthracene-9,10-diyl)bis(ethyne-2,1-diyl))bis(triisopropylsilane), ***5***

In a 20 mL vial, 300 mg of **2** (0.39 mmol) and 200 mg of $SnCl_2$ were suspended in 20 mL of methanol and 0.2 mL of HCl 12 M were added. The color of the stirring solid rapidly changed to orange and became fluorescent. The reaction was left in the dark at 70°C for 1 hour. The content was then poured in water, the solid filtered, washed abundantly with water and dried. It was then dissolved in dichloromethane and passed through a 0.22 µm Teflon filter to remove any possible tin residue and the solvent was removed under vacuum. The product was obtained as an orange solid (267 mg, 97% yield). ^{1}H NMR (400 MHz, $CDCl_3$) δ (ppm): 8.83 (d, *J* = 2.0 Hz, 1H), 8.47 (d, *J* = 9.1 Hz, 1H), 7.69 (dd, *J* = 9.2, 2.0 Hz, 1H), 1.29 (d, *J* = 5.3 Hz, 21H). The signals were comparable to those reported by Park et al..[3]

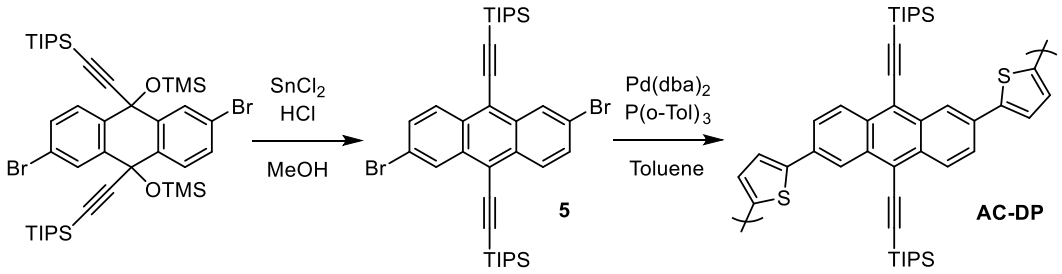

Stille polymerization of ***5*** *and 5,5'-bis(trimethylstannyl)-2,2'-bithiophene,* ***AC-DP***

A similar procedure for the polymerization of **AQ-DP** reported above was followed. In a dry 50 mL Schenk under argon, 120 mg of **5** (0.17 mmol, 1 Eq) and 141 mg of 5,5'-bis(trimethylstannyl)-2,2'-bithiophene (0.29 mmol, 1.05 Eq) were dissolved in 20 mL of dry toluene and the solution degassed. 16 mg of bis(dibenzylideneacetone)palladium(0) (0.03, 0.1 Eq) and 34 mg of tri(o-toluyl)phosphine (0.12 mmol, 0.4 Eq) were added and the reaction left at 110 °C for 1.5 hour. Longer reaction times resulted in the formation of a large fraction of intractable solid. Initially, the solution was blue fluorescent, which then turned to yellow and, after 1 hour, it was not detectable anymore. 0.2 mL of 4-tertbutyl-1-bromobenzene were added and the reaction left for one additional hour. The solution was then poured in 200 mL of methanol and the precipitate extracted with hot acetone and hot chloroform. The chloroform fraction was precipitated in methanol to obtain a brown powder (19 mg, 16% yield). The IR spectrum shown in Figure 1 was taken on the non-soluble fraction after washing with boiling acetone and chloroform. Mn= 1302 Da, Mw= 1606 Da, PDI= 1.23.

Synthesis of ((2,6-di(thiophen-2-yl)-9,10-bis((triisopropylsilyl)ethynyl)-9,10-dihydroanthracene-9,10-diyl)bis(oxy))bis(trimethylsilane), ***AH-Model***

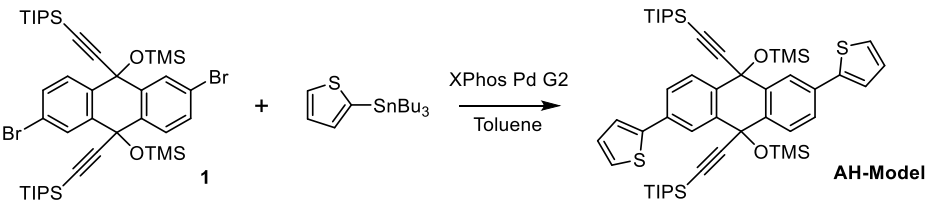

In a dry 25 mL flask under nitrogen, 500 mg of 1 (0.57mmol, 1 Eq) were dissolved in 10 mL of dry toluene and the solution degassed. 0.53 mL of 2-(tributylstannyl)thiophene (1.43 mmol, 2.5 Eq) and 47 mg of X Phos Pd G2 (0.06 mmol, 0.1 Eq) were added and the reaction left at 120°C for 6 hours. It was then diluted with

chloroform and extracted with water. The organic phase was dried over $MgSO_4$ and the solvent removed under vacuum. The product was recrystallized from ethyl acetate and obtained as pale yellow crystals (252 mg, 50% yield). ^{1}H NMR (400 MHz, Chloroform-d) δ (ppm): 8.24 (d, *J* = 2.0 Hz, 1H), 7.98 (d, *J* = 8.3 Hz, 1H), 7.69 (dd, *J* = 8.3, 2.1 Hz, 1H), 7.45 (dd, *J* = 3.6, 1.2 Hz, 1H), 7.34 (dd, *J* = 5.1, 1.1 Hz, 1H), 7.14 (dd, *J* = 5.1, 3.6 Hz, 1H), 1.17 – 1.01 (m, 21H), -0.25 (s, 9H). ^{13}C NMR (101 MHz, Chloroform-d) δ (ppm): 144.04, 137.45, 136.01, 134.42, 129.96, 128.13, 126.35, 125.97, 125.08, 123.30, 112.10, 86.28, 68.45, 18.73, 11.39, 1.54. Elem. Anal. $C_{50}H_{72}S_2O_2Si_4$ Calc. (%) C 68.12 H 8.23 S 7.27 O 3.63 Si 12.74. Exp. (%) C 67.92 H 8.214 S 7.17. NMR spectra be are shown in Figures S13-S15.

Synthesis of ***AC-Model*** *from* ***AH-Model***

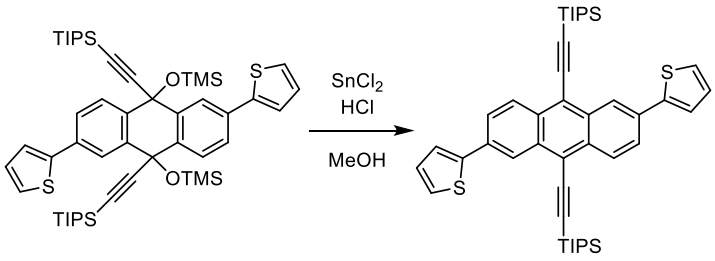

In a 20 mL vial, 30 mg of **AH-Model** (0.03 mmol) were suspended in 2 mL of methanol and placed at 60°C. A solution of 50 mg of $SnCl_2$ in 8 mL of methanol containing 0.1 mL of HCl 12 M was added and the reaction left under stirring for 1 hour. The solution rapidly changes color and orange precipitate forms. It was filtered and washed abundantly with water and briefly with methanol. 23 mg of product as an orange powder were collected (97% yield). ^{1}H NMR (400 MHz, Chloroform-d) δ (ppm): 8.93 – 8.80 (m, 1H), 8.60 (dd, *J* = 9.0, 0.7 Hz, 1H), 7.89 (dd, *J* = 9.0, 1.9 Hz, 1H), 7.53 (dd, *J* = 3.6, 1.1 Hz, 1H), 7.37 (dd, *J* = 5.1, 1.1 Hz, 1H), 7.15 (dd, *J* = 5.1, 3.6 Hz, 1H), 1.43 – 0.99 (m, 21H). ^{13}C NMR (101 MHz, Chloroform-d) δ (ppm): 144.41, 132.66, 132.57, 132.28, 128.37, 128.02, 125.88, 125.83, 124.10, 123.06, 118.63, 105.37, 103.18, 19.10, 11.63. Elem. Anal. $C_{44}H_{54}S_2Si_2$ Calc. (%) C 75.15 H 7.74 S 9.12 Si 7.99. Exp. (%) C 75.55 H 7.597 S 9.088. NMR spectra be are shown in Figures S13-S15.

Synthesis of ***AQ-Model*** *from* ***AH-Model***

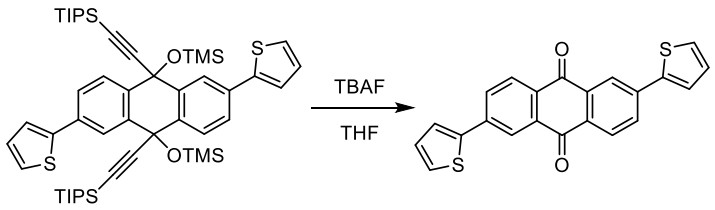

In a 50 mL Schenk, 50 mg of **AH-Model** (0.07 mmol, 1 Eq) were dissolved in 30 mL of THF and 0.42 mL of TBAF 1 M solution in THF (0.42 mmol, 6 Eq) were added. The solution was heated to 80 °C for 1 hour until it turned dark green. The solvent was then removed in vacuum and the leftover brown solid washed abundantly with water. 25 mg of product as an orange powder were collected (96% yield). ^{1}H NMR (400 MHz, Chloroform-d) δ (ppm): 8.55 (d, *J* = 2.0 Hz, 1H), 8.35 (d, *J* = 8.1 Hz, 1H), 8.02 (dd, *J* = 8.2, 2.0 Hz, 1H), 7.62 (dd, *J* = 3.7, 1.1 Hz, 1H), 7.48 (dd, *J* = 5.1, 1.1 Hz, 1H), 7.20 (dd, *J* = 5.1, 3.7 Hz, 1H). ^{13}C NMR (101 MHz, Chloroform-d) δ (ppm): 182.43, 142.18, 140.13, 134.23, 131.94, 130.48, 128.66, 128.34, 127.51, 125.67, 123.79. The signal are compatible with those reported by Birajdar et al..[4] NMR spectra can be are shown in Figures S13-S15.

*Example of synthesis of **AC-P** from **AH-P***

In a vial, 50 mg of **AH-P** were suspended in 10 mL of a solution containing 50 mg of $SnCl_2$ and 0.1 mL of HCL 37% at 50°C for 3 min. Immediately the polymer turned red and dim red fluorescence could be detected. The solid was then filtered and washed abundantly with methanol, water and acetone. The obtained material (37 mg, 98% yield) was insoluble and characterized via IR (Figures 1 and SI7) and elemental analysis. ^{13}C ssNMR is shown in Figure SI6. Elem. Anal. $C_{44}H_{52}S_2Si_2$ Calc. (%) C 75.37 H 7.48 S 9.14 Si 8.01. Exp. (%) C 71.11 H 7.680 S 8.716.

*Example of synthesis of **AQ-P** from **AH-P***

In a vial, 50 mg of **AH-P** were added to 5 mL of a 0.2 M TBAF solution in THF ant the reaction was left for 5 minutes. Brown precipitate forms which was filtered and washed abundantly with water and acetone. The obtained material (21 mg, 99% yield) was insoluble and characterized via IR (Figures 1 and SI7) and elemental analysis. ^{13}C ssNMR is shown in Figure SI6. Elem. Anal. $C_{22}H_{10}O_2S_2$ Calc. (%) C 71.33 H 2.72 O 8.64 S 17.31 Exp. (%) C 69.66 H 2.939 N 0.01 S 16.423.

Discussion and comments on the transformation reactions

Reduction-rearomatization reactions. Among the several conditions tested the better performing one was to employ a solution of 50 or 100 mg of $SnCl_2$ in 10 mL of methanol and 0.1 mL of HCl 37%. The product formed employing these conditions required no purification except washing with abundant water and methanol. An example of the outcome of this reaction can be found in Figure SI2 where the ^1H-NMR spectrum of **5** is compared to that of **1** and 2,6-dibromoanthraquinone. Employing sulfuric acid seemed to slow down the reaction while employing THF:water or THF:methanol solvent mixtures (other common solvents for the reduction-rearomatization reactions) resulted in more byproducts. The same reaction was tested on **AH-Model** to form **AC-Model** (as reported above). The result was similar and the ^1H-NMR of this compound is compared to that of **AH-Model** and the **AQ**-containing analogue in Figures SI3 through SI5. Even in this case, no purification procedure was performed except washing with water. The different pattern in the aromatic region and the absence of the signal related to the TMS protons is obvious.

The same reaction conditions were applied to **AH-P** resulting in the conversion to the desired **AC-P**. This transformation was monitored via ^{13}C-ssNMR and IR because of the insolubility of the polymer. By comparison with the ^{13}C-NMR of **AH-P** (Figure SI6), the former strongly indicates the presence of aromatic and TIPS carbons, as expected from the structure. The IR corroborate such observation (Figure SI7) with the disappearance of the several signals in the 1000-1400 cm^{-1} region ascribable to C-O-Si$(CH_3)_3$. Figure 1 in the main text also shows the similarity between the polymer obtained via the precursor route and the one obtained through direct polymerization.

As **AH-P** is not soluble in methanol, the same reaction can be run on thin polymer films. When we employed ITO substrates, however, a saturated solution of $SnCl_2$ in acetic acid was employed for the transformation since HCl rapidly degrades the ITO layer. (For our ITO substrates, boiling in neat acetic acid for 3 h only reduced the conductivity of about 20%.) The reaction still works (similar yields are found for the reduction-rearomatization of **1** in these conditions) but the kinetics are slower.

Retro-Favorskii reactions. Initially, we tested the reactivity of the monomers in common retro-Favorskii conditions (KOH, toluene, 110°C). With the exception of substrates comprising an OH group on the propargyl

alcohol moiety (obtained by treating the related TMS-protected compounds with K_2CO_3 in methanol overnight) which reacted quite fast (<1h), 6 hours were needed in the case of compounds **1** and **4**, while **2** did not react (Figure SI9). These reactions time are not compatible with the fabrication needs. Interestingly, as mentioned in the main text, we found that the fluoride ion without protic sources can act as a strong base and perform this reaction fast and with high yields. We wrote a detailed report about the use of tetrabutylammonium fluoride (TBAF) as reagent for this type of reactions which can be found at 10.26434/chemrxiv-2023-bm7dl. Remarkably, the transformation was tolerant to humidity and no anhydrous conditions were required. An example reaction on **1** and **AH-Model** consisted of dissolving the material in THF and adding an excess of TBAF as TBAF solution 1M in THF and leaving the reaction at 80°C until the color of the solution became dark (within minutes; a detail recipe was mentioned above). We report the ^{1}H-NMR of the products obtained from these reactions (with no further purification than extended washing with water and – if necessary – acetone) in Figures SI2 to SI5.

A similar procedure can also be applied to **AH-P**. For the latter, the outcome of the reaction was investigated as described previously in the case of **AC-P**. In this case, the ^{13}C-ssNMR (Figure SI6) showed signals that one could ascribe to the formation of carbonyl groups. In contrast, the signals of the carbons bound to Si – expected to be characterized by a high intensity in a magnetization transfer experiment because of the vicinity of many protons – almost – completely disappeared. The IR spectrum (Figure SI7) also shows a noticeable change, developing the characteristics signals of 2,6-anthraquinoid compounds. The confrontation of the IR spectrum of **AQ-P** with that of its analogue obtained via direct polymerization (**AQ-DP**) in Figure 1 in the main text clearly show that they are superimposable.

One of the main advantages of using TBAF is that it can be dissolved in several organic solvents and thus the transformation of the precursor polymers to **AQ-P** can be carried out in several different conditions. In particular, if ketonic solvents (such as acetone or methylisobutylketone, MIBK) were employed, the transformation happened without the dissolution of the precurosor, thus forming **AQ-P** from the precursor in the solid state. To avoid the use of THF (which dissolves **AH-P**), we employed either acetone or MIBK, which can be used to dissolve TBAF hydrate or to dilute a more practical TBAF solution in THF so that THF does not act as a solvent anymore. Generally, we employed 4:1 ketonic solvent:1 M TBAF solution in THF mixtures. It is worth noting that these solutions should be prepared fresh as the basic character of the fluoride ion in these conditions can generate enolization products over a matter of hours, especially if they are heated, recognizable by the appearance of a brown coloration in the solutions.

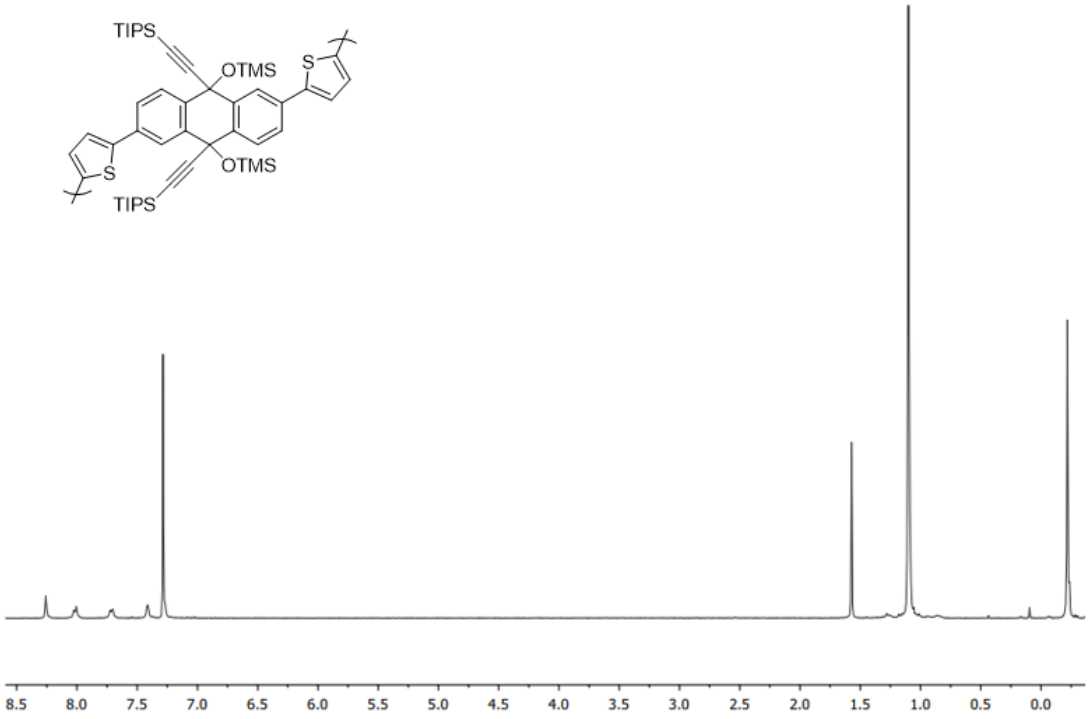

Figure SI1. ^{1}H NMR spectrum of **AH-P**

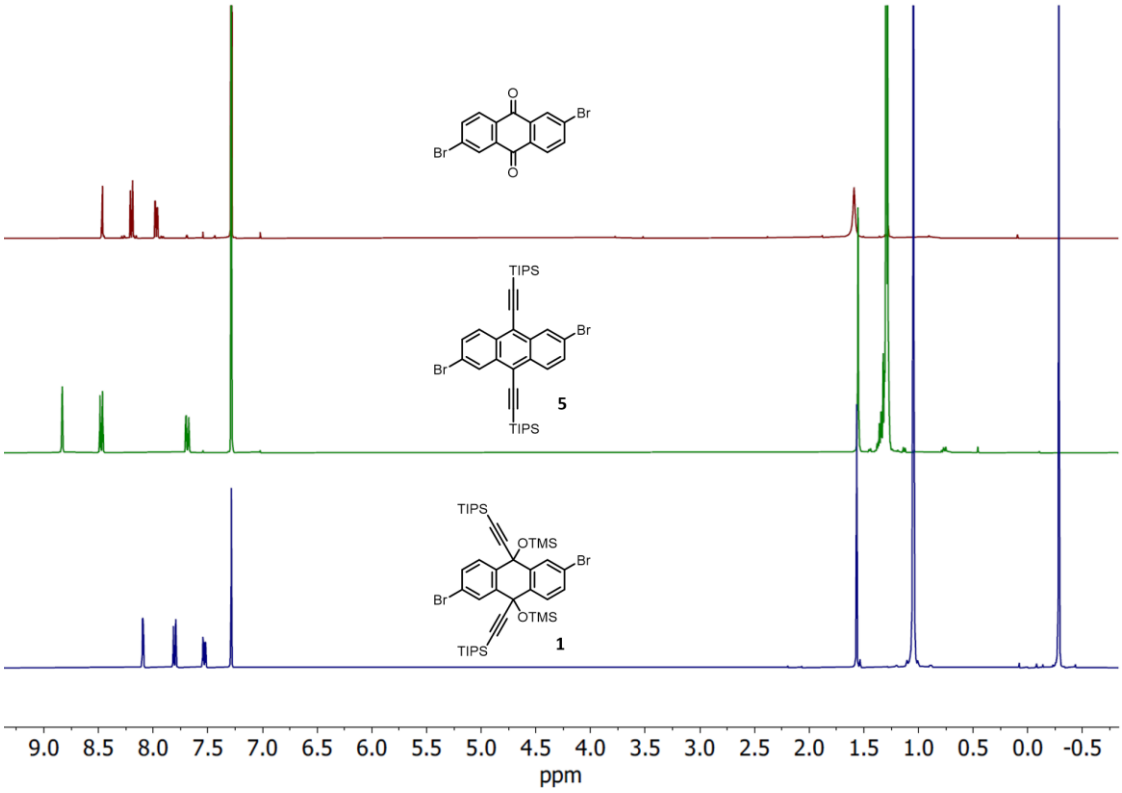

Figure SI2. Comparison of ^{1}H NMR spectra of **1** (blue), 2,6-dibromoanthraquinone (obtained from **1** via fluoride-promoted retro-Favroskii reaction; red), and **5** (obtained from **1** via reduction-rearomatization; green).

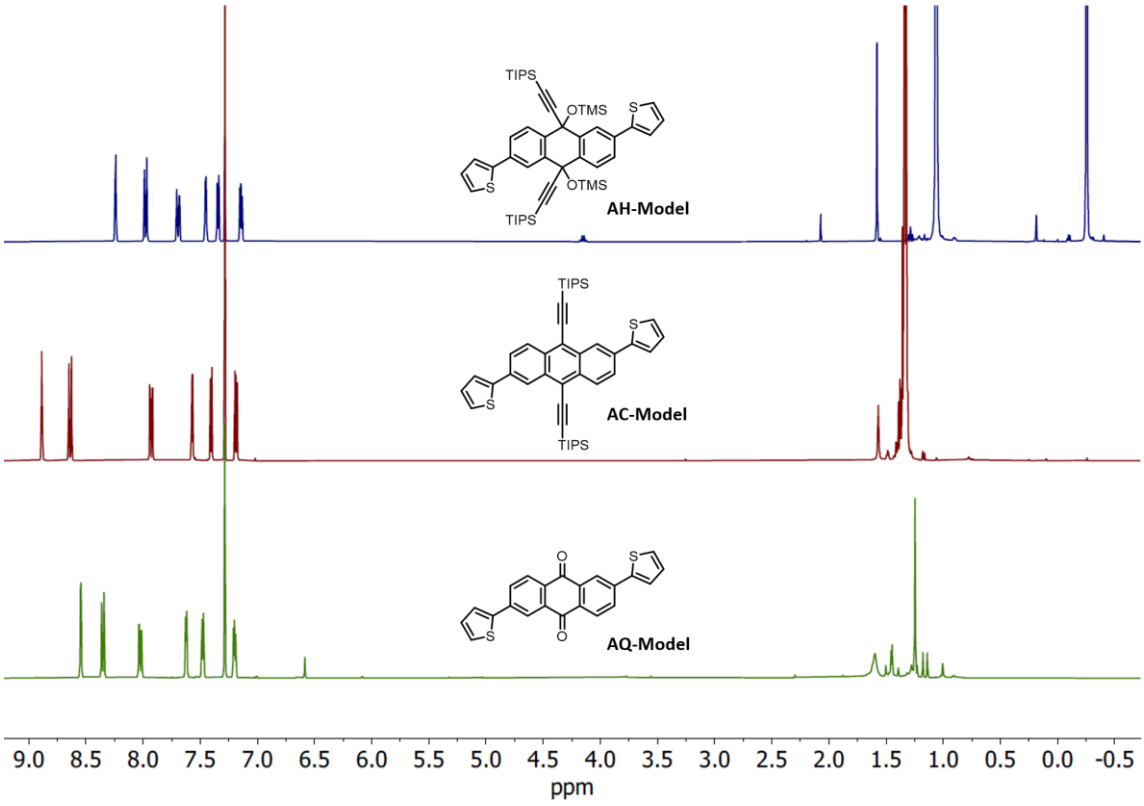

Figure SI3. Comparison of ^{1}H NMR spectra of **AH-Model** (blue), **AC-Model** (red), and **AQ-Model** (green). Signals in the aliphatic part of the latter spectrum are impurities that were not washed with water.

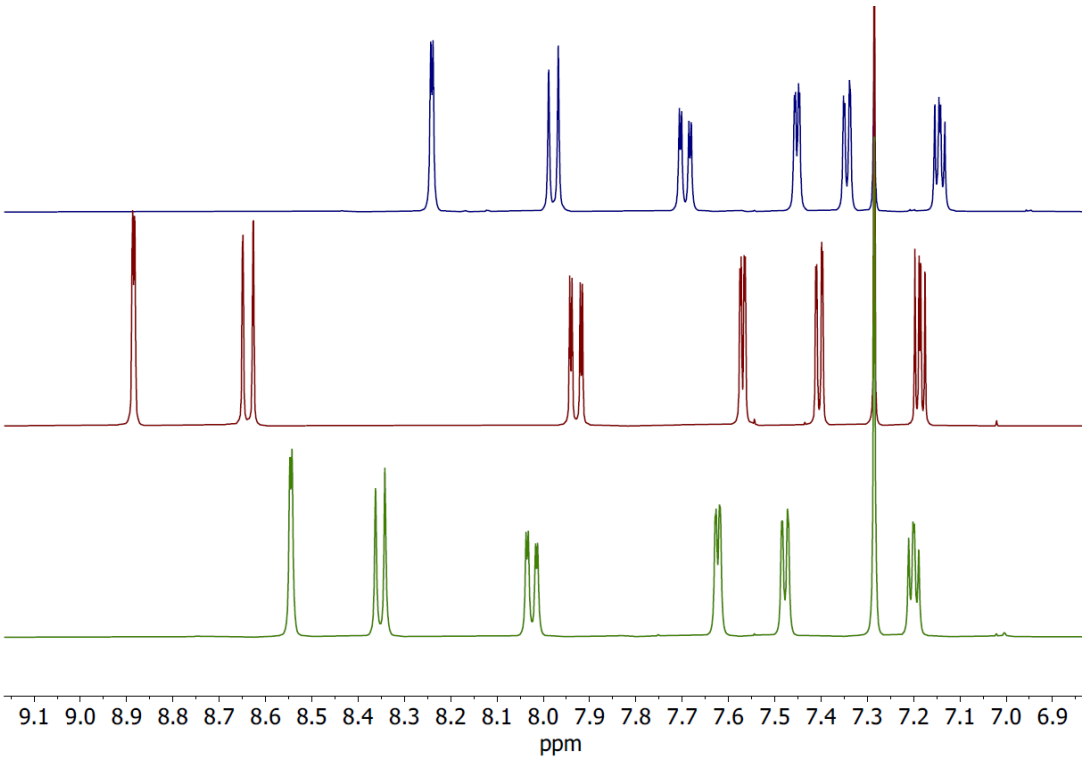

Figure SI4. Expansion of the aromatic peaks of the previous spectra.

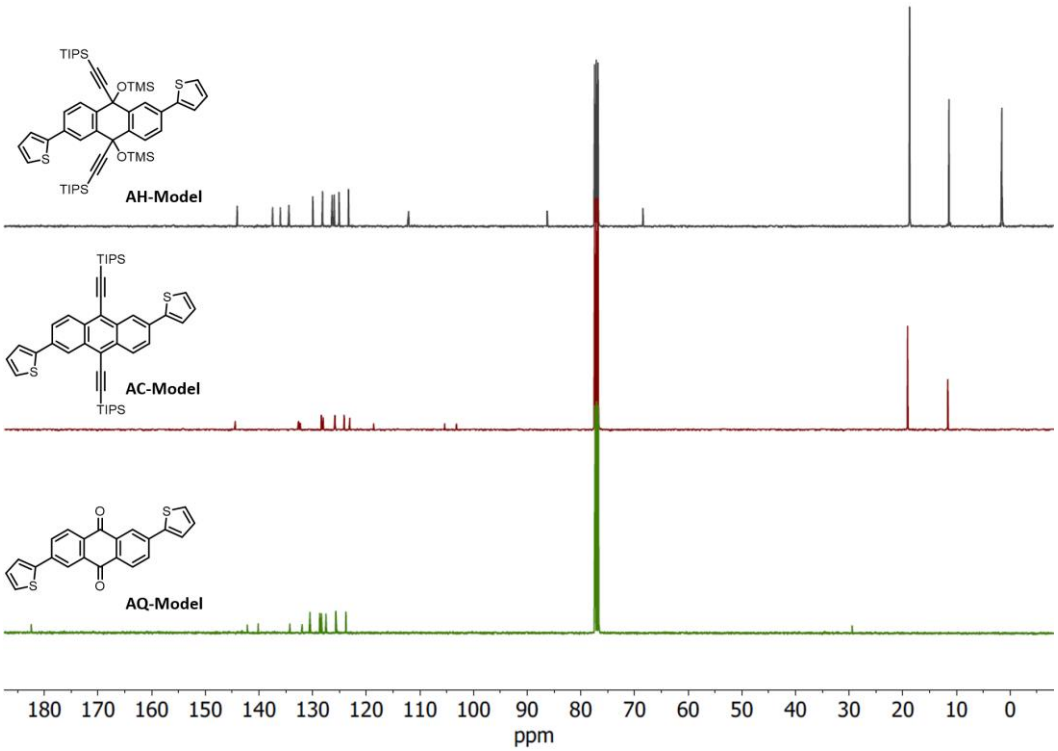

Figure SI5. Comparison of ^{13}C-NMR spectra of **AH-Model** (top), **AC-Model** (middle), and **AQ-Model** (bottom).

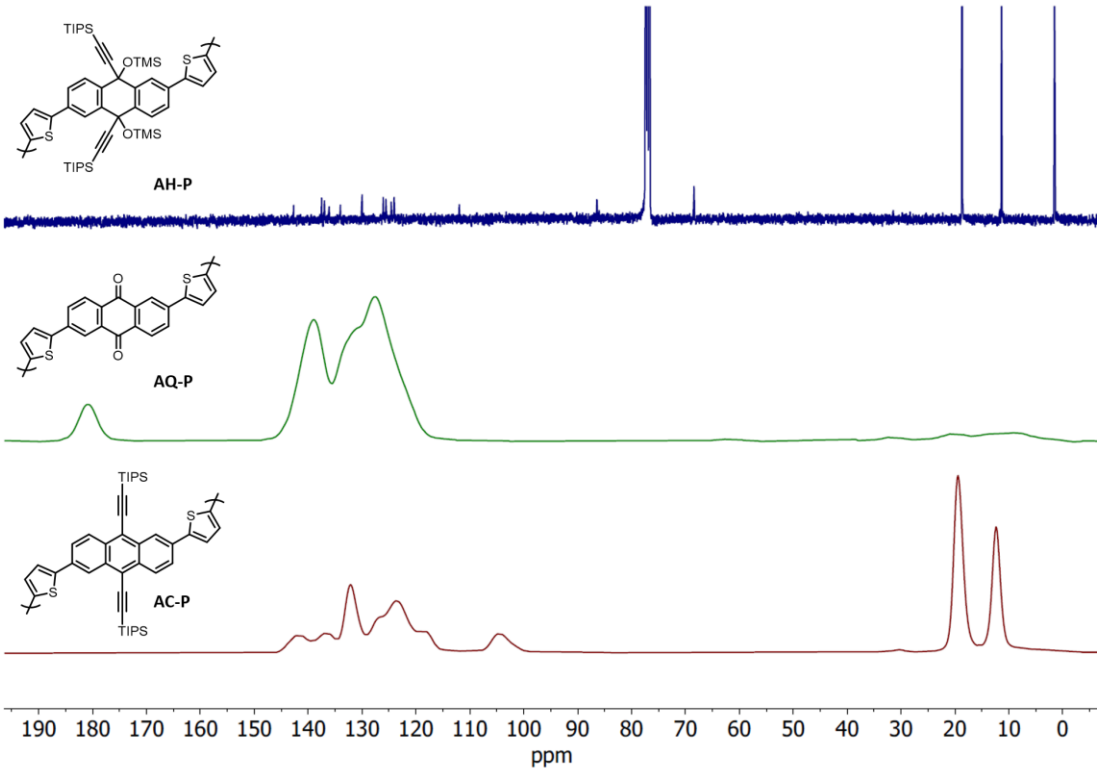

Figure SI6. Comparison between ^{13}C-NMR (in $CDCl_3$) of **AH-P** (top) and the ^{13}C-ssNMR of **AQ-P** (middle) and **AC-P** (bottom).

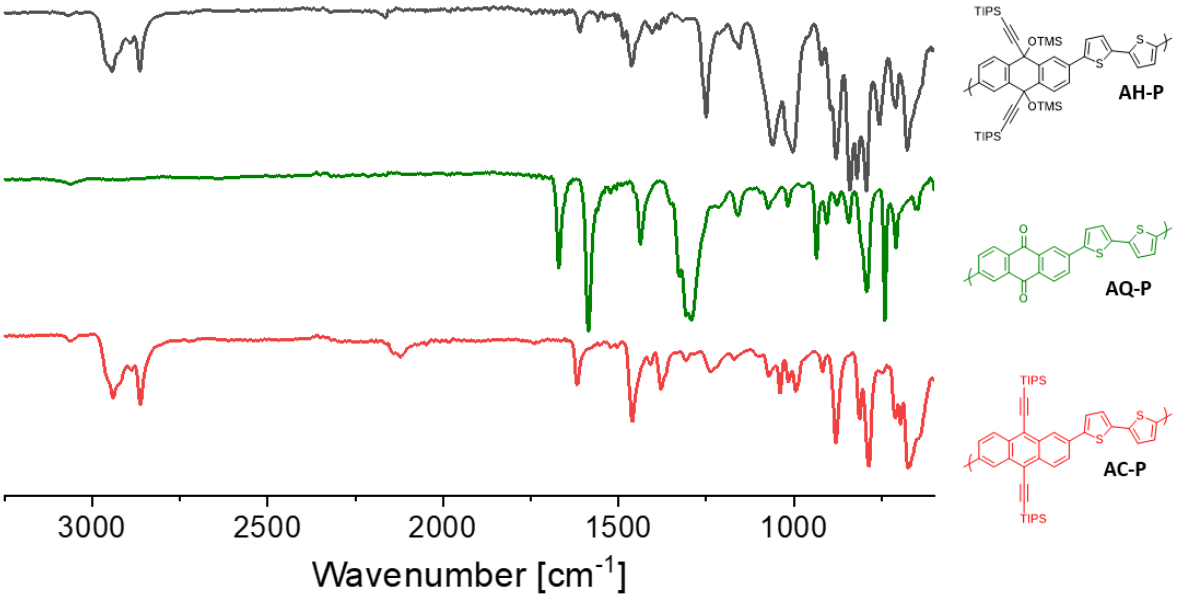

Figure SI7. Comparison between IR-ATR spectra of **AH-P**, **AQ-P**, and **AC-P**.

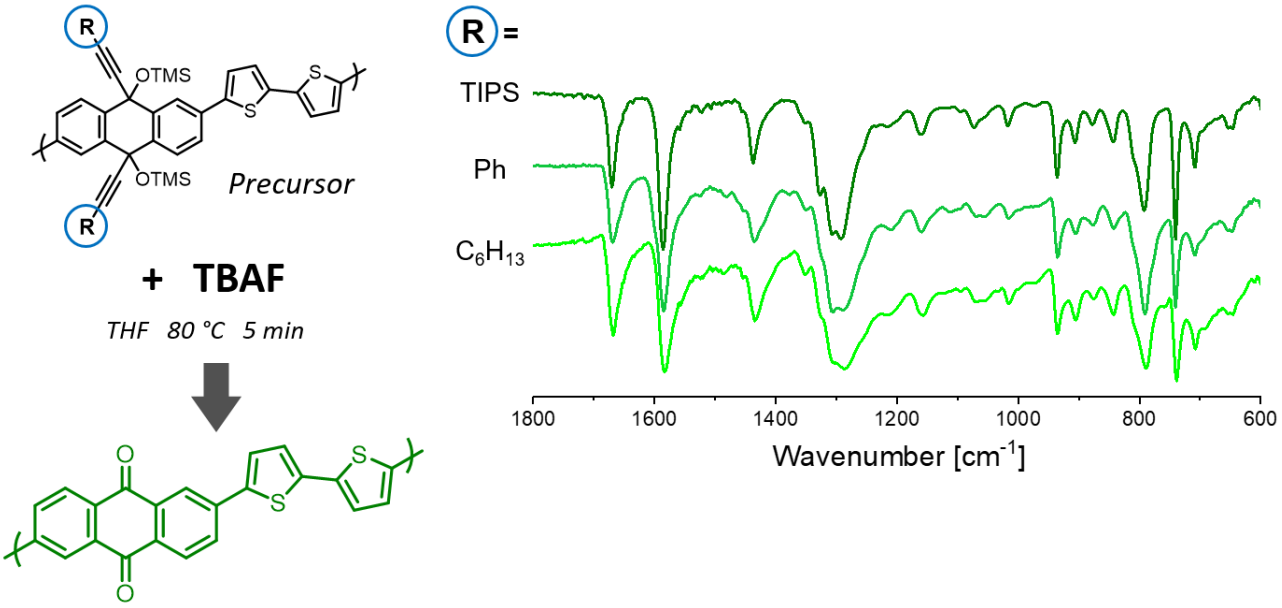

Figure SI8. Comparison between IR-ATR spectra of **AQ-P** obtained from **AH-P**, **3-P**, and **4-P** via an identical reaction. **2-P** does not react in such conditions.

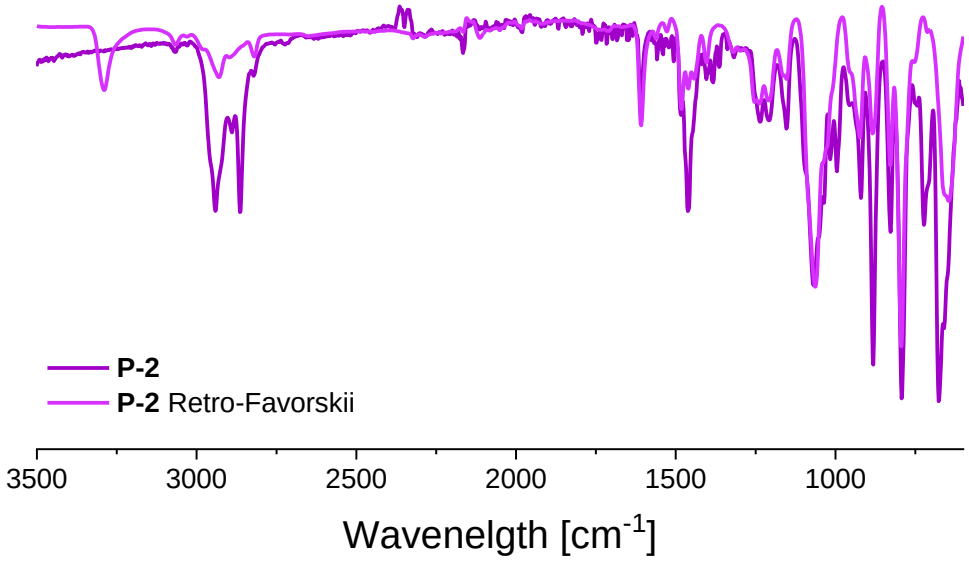

Figure SI9. Comparison between IR-ATR spectra of **2-P** and **2-P** treated in fluoride retro-Favorskii conditions (10 mg of polymer in 5mL TBAF 0.2 M in THF; closed vial 100°C; 4 hours). The spectral profiles are very similar except for the region above 2800 cm^{-1} which indicates a loss of TIPS protons and an appearance of a terminal alkyne C-H bond.

Thin Film characterization

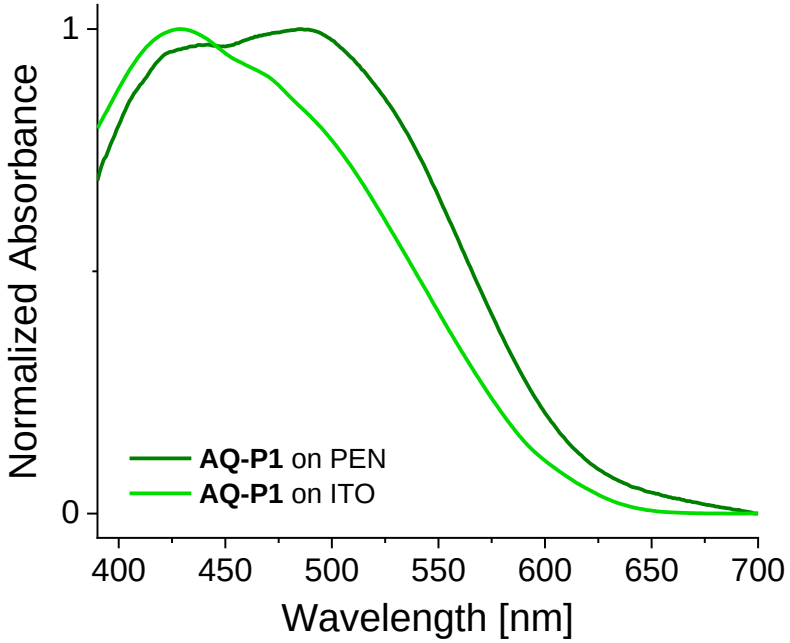

Figure SI10. Comparison between UV-Vis absorption of **AQ-P** (from **AH-P**) films on PEN and ITO substrates.

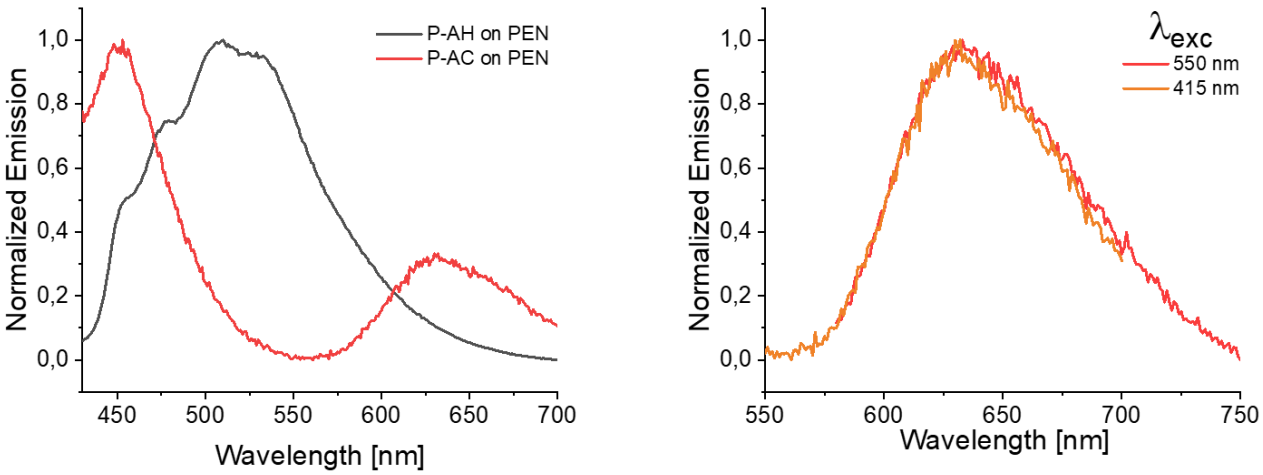

Figure SI11. Left: Normalized fluorescence spectra of **P-AH** (black) and **P-AC** (red) on PEN substrates. (The peak centered at 450 nm is the fluorescence of the PEN substrate.) Right: Comparison of the emission of the **P-AC** film upon excitation at different wavelengths.

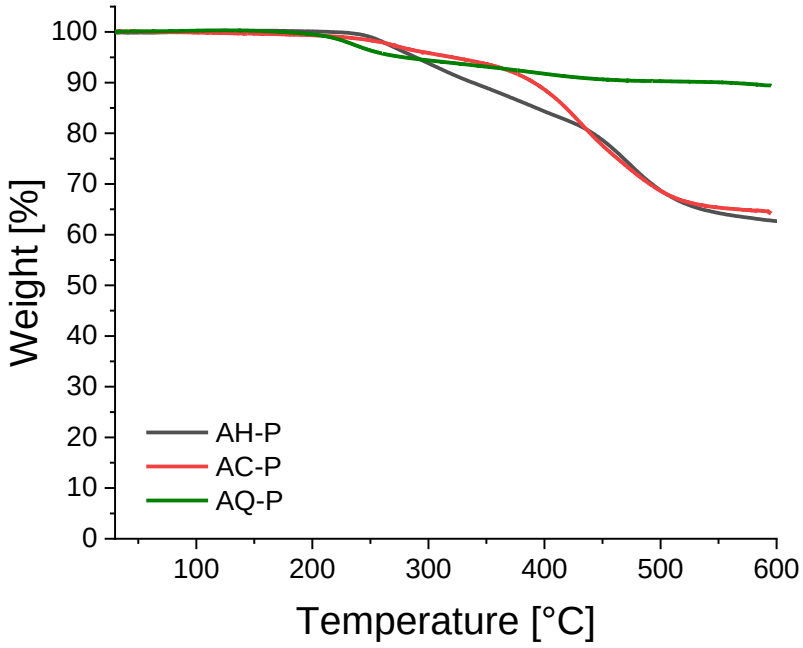

Figure SI12. TGA curves of the polymers.

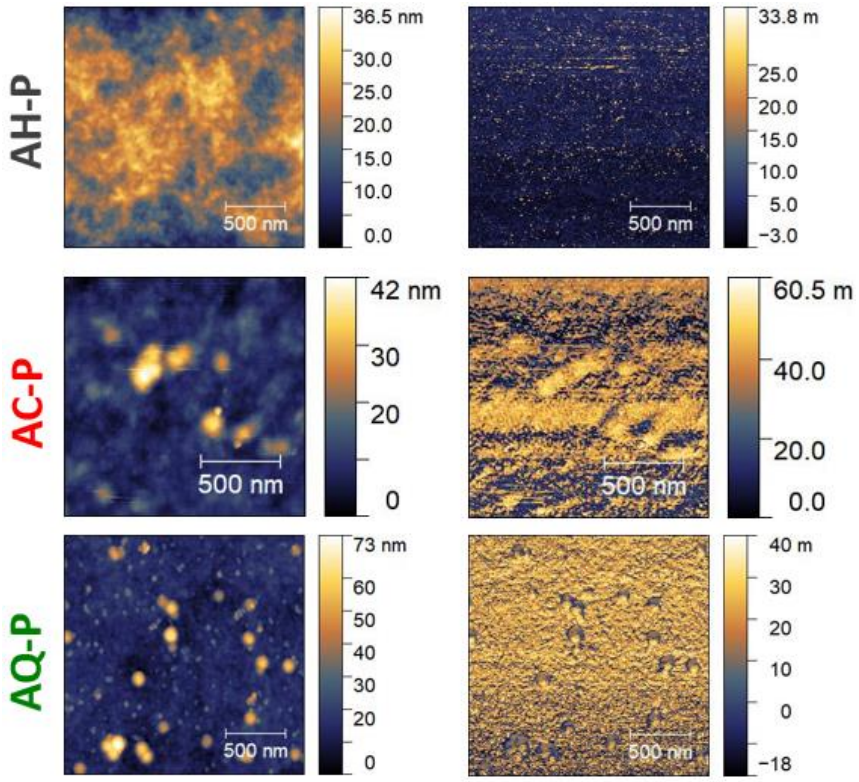

Figure SI13. AFM height (right) and phase (left) spectra of thin films of **AH-P**, **AC-P**, and **AQ-P** obtained via spin coating from a 15 mg/mL o-dichlorobenzene solution on PEN (1000 rpm, 60 s, acceleration 500 ms).

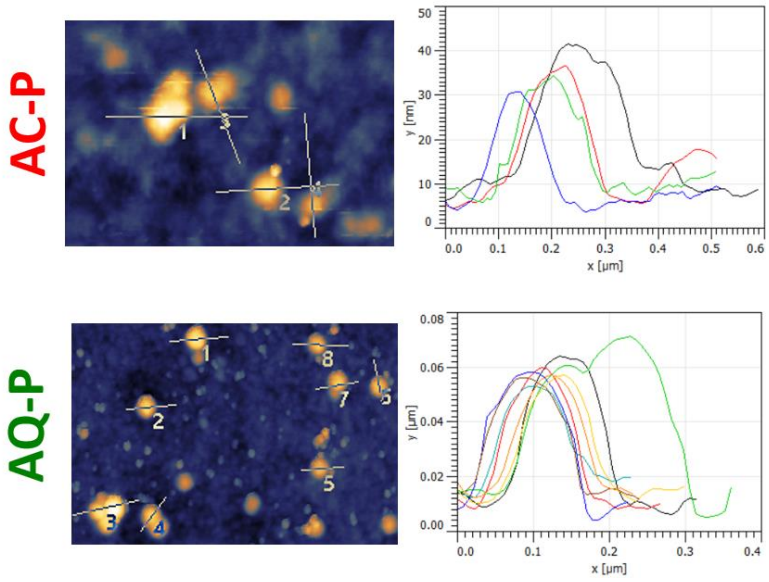

Figure SI14. Analysis of the different particles observed in the AFM scans.

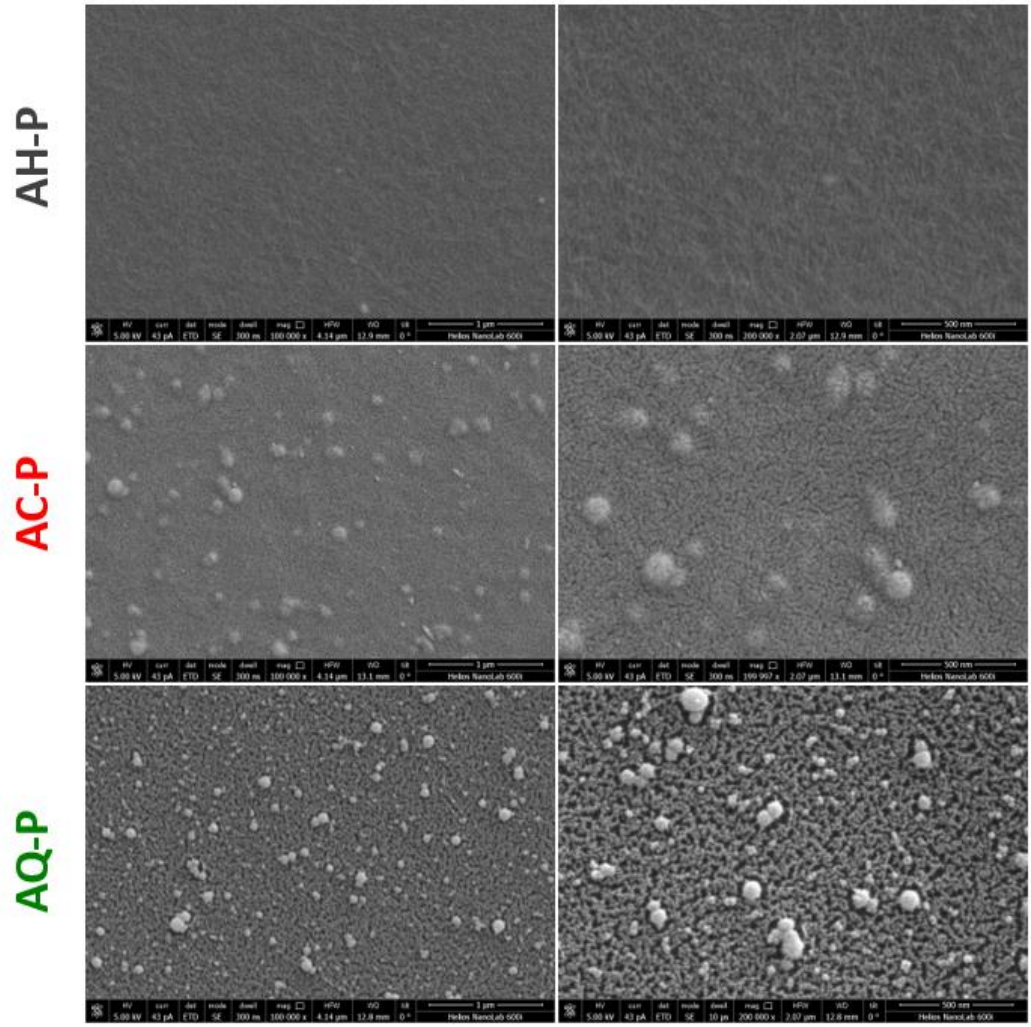

Figure SI15. SEM images of **AH-P** (top), **AC-P** (middle), and **AQ-P** (bottom) at different magnifications.

XPS data

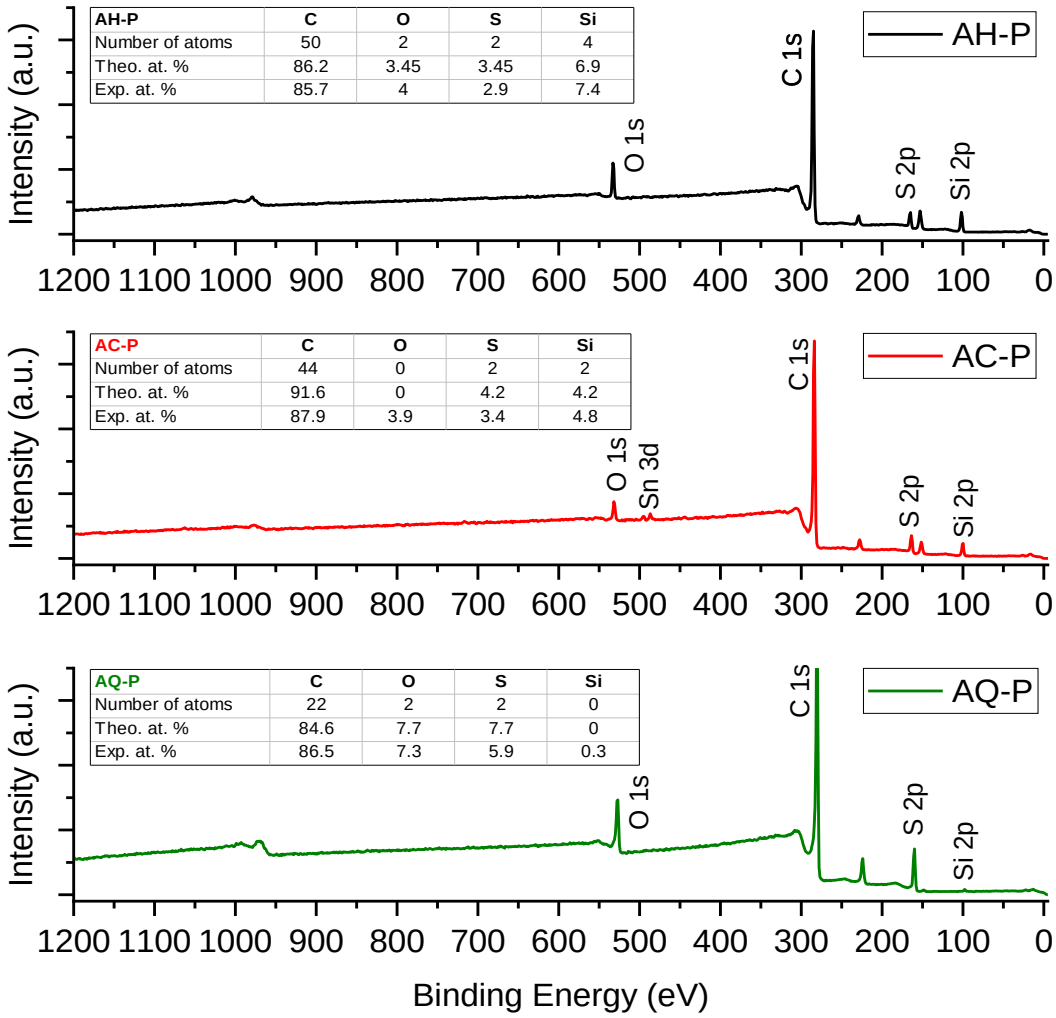

Figure SI16. XPS wide scans of **AH-P**, **AC-P**, and **AQ-P**, respectively. A table reporting the number of atoms per monomeric unit, the theoretical atomic percentage (theo. at. %), and the XPS-determined atomic percentage (exp. at. %) of C, O, S, and Si is reported for the samples. The main XPS peaks for the elements observed on each sample are labelled in the spectra.

UPS data

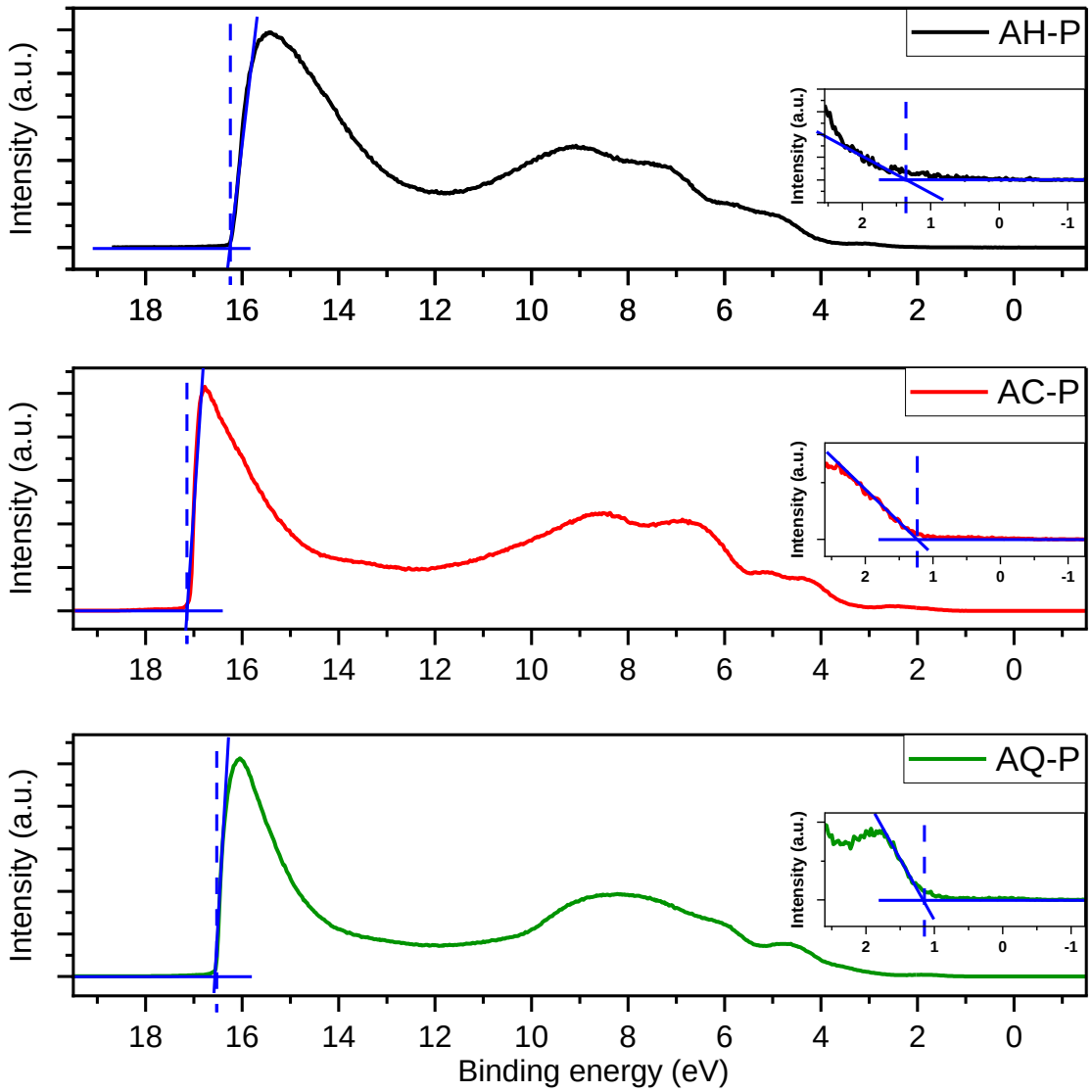

Figure SI17. UPS spectra of **AH-P**, **AC-P**, and **AQ-P**, respectively. Insets highlight the onset energies.

Voltammograms

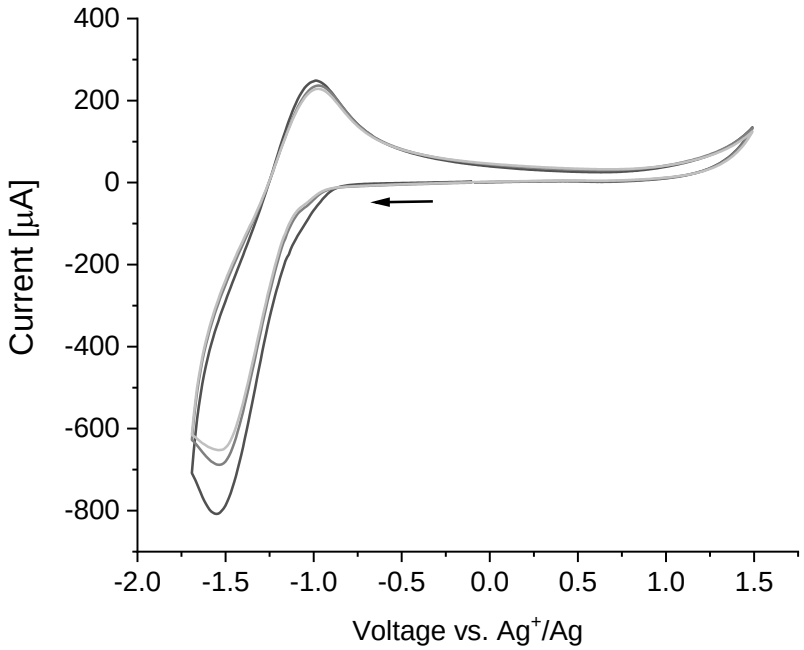

Figure SI18. Voltammograms (3 scans; from black to light grey) of a film of **AQ-P** on ITO (0 V → -1.5 V → 1.5 V; 0.1V/s). The reference is described in the Materials and Methods section.

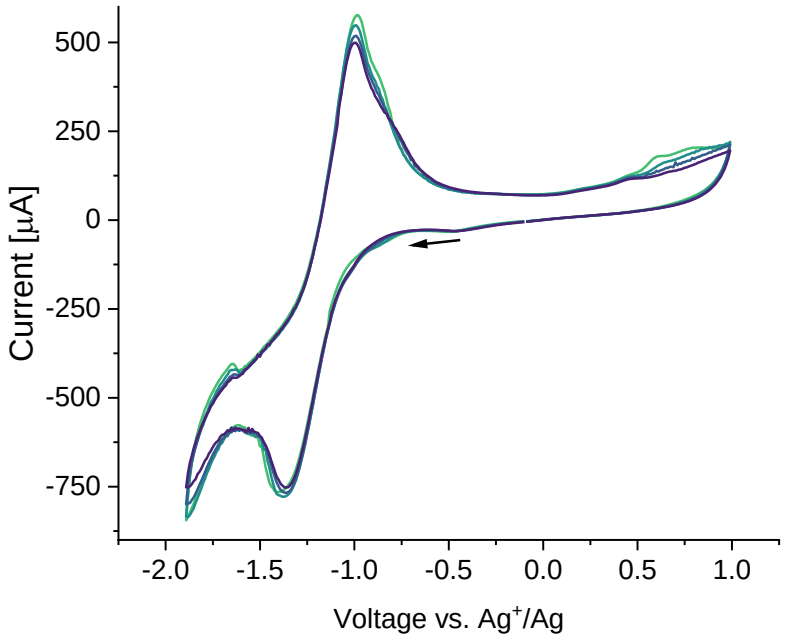

Figure SI19. Voltammograms (5 scans; from green to blue) of a film of **AQ-P** on Au (0 V → -1.9 V → 1 V). The reference is described in the Materials and Methods section.

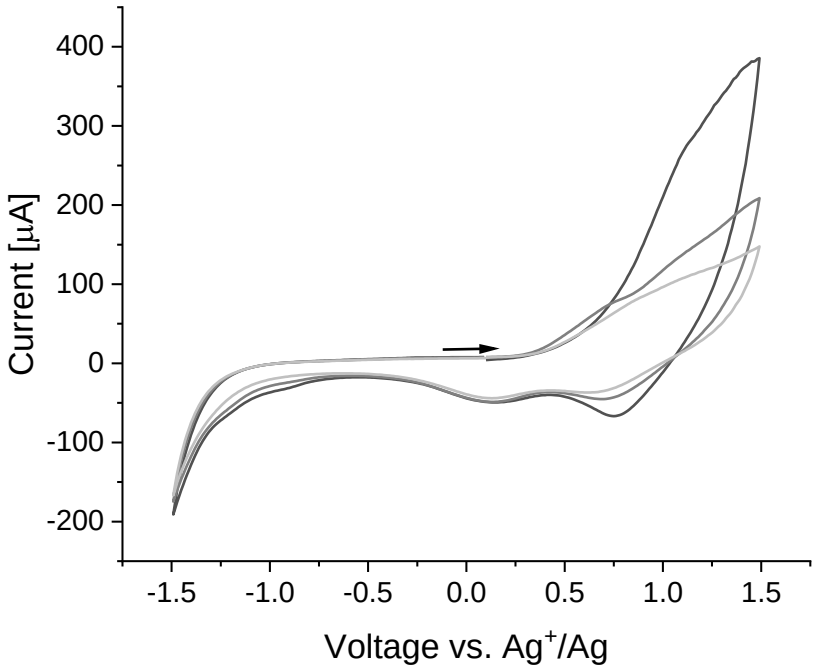

Figure SI20. Voltammograms (5 scans; from black to light grey) of a film of **AC-P** on ITO (0 V → 1.5 V → -1.5 V; 0.1V/s). The reference is described in the Materials and Methods section.

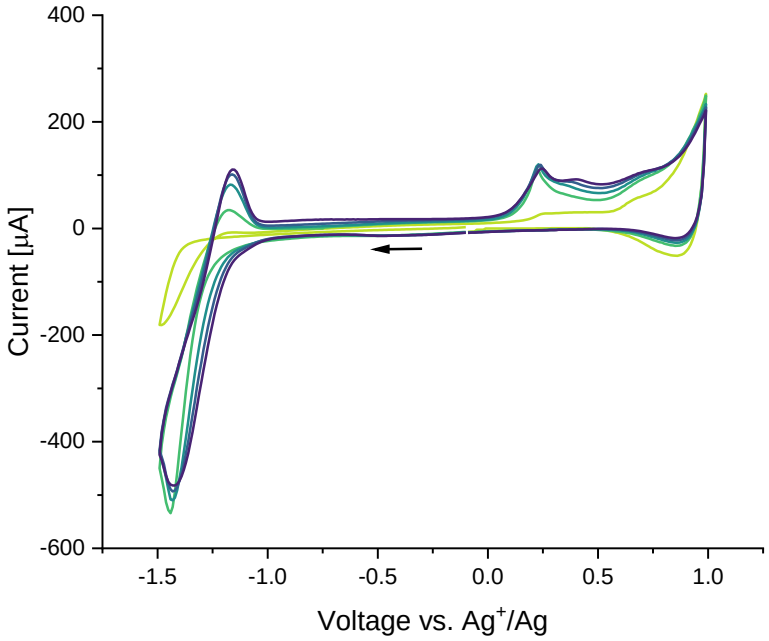

Figure SI21. Voltammograms (5 scans; from green to blue) of a film of **AC-P** on Au (0 V → -1.5 V → 1.5 V; 0.1V/s). The reference is described in the Materials and Methods section. The large difference between scan 1 (dark yellow) and 2 (green) clearly indicates that the reduction peak at -1.4 V and the irreversible oxidation peak at 0.2 V result from possible reactions in the film upon oxidation.

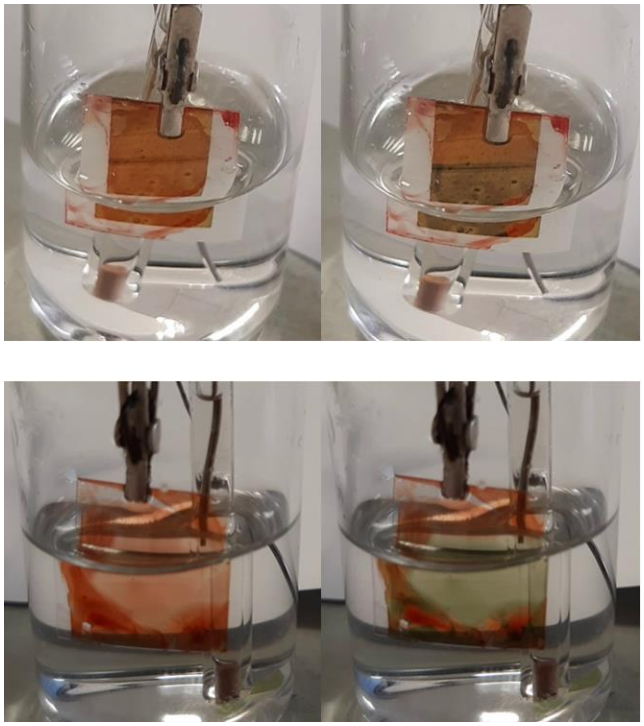

Figure SI22. Pictures of the color change of a film of **AC-P** on Au upon oxidation (top) and of a film of **AQ-P** on ITO upon reduction (bottom).

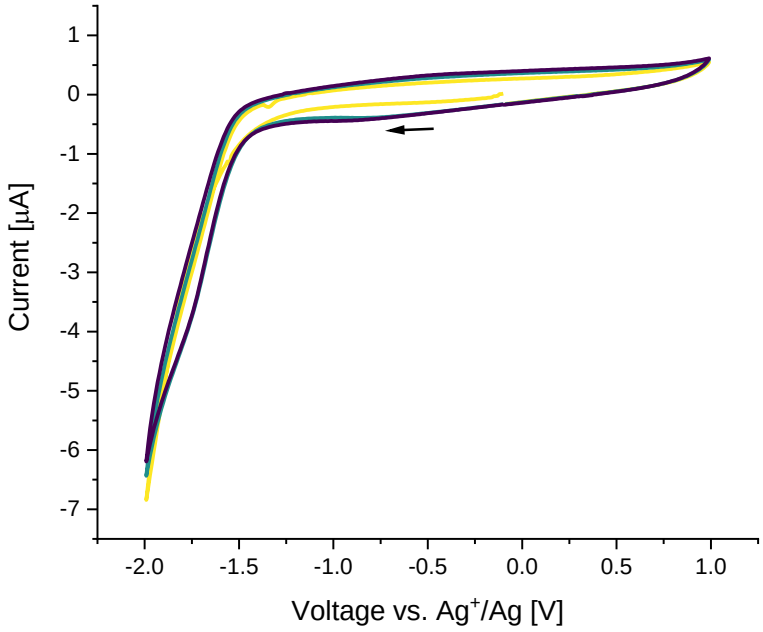

Figure SI23. Voltammograms (5 scans; from green to blue) of a film of **AH-P** on Au (0 V → -1.5 V → 1 V; 0.1V/s). Despite the similar active surfaces employed, the currents are two orders of magnitude smaller in this case.

Spectroscopic analysis of the reduction of AQ-P films

An ITO-covered glass slide (2x1x0.11 cm; 20 Ω sq; IJ Cambria Scientific Ltd, UK) was dip coated in a solution of **AH-P** 15 mg/mL in o-dichlorobenzene (enough to cover the bottom half) and let dry. The sample was then immersed in 2.5 mL of a MIBK:TBAF 1M in THF 4:1 solution at 100°C and left for 3 minutes. It was then washed with abundant methanol, water, methanol, and acetone (direct immersion in water may result in the detachment of the film from the ITO) and dried on a hotplate at 120°C for 1 hour. Conductive copper tape was then placed on the exposed ITO and connected to the potentiostat. The sample, the counter electrode (Pt wire) and a reference Ag wire were immersed in a quartz cuvette filled with degassed acetronitrile and 0.1 M Bu_4NPF_6. After a preliminary CV scan to observe the reduction peak with the new reference, we performed a slow scan (0.001V/s) between -0.5 V → -1.2 V → -0.5 V while recording absorption spectra continuously. The results of this measurement are shown in Figure 3 in the main text.

Multicolored Electrochromic Display

A solution of **AH-P** 15 mg/mL in o-dichlorobenzene was spun coated (1000 rpm, 60 s, acceleration 500 ms) on an ITO-coated PET substrate (30-60 Ω sq; Sigma-Aldrich, UK) and dried at 120°C for 1 hour. It was then placed on a hotplate at 80°C and two rubber stamps (siloxane) were employed to transfer in a controlled manner small quantities of either a saturated solution of $SnCl_2$ in acetic acid or a MIBK:TBAF 1M in THF 4:1 solution on the film to prepare regions of **AC-P** and **AQ-P**, respectively. The substrate was then washed abundantly with methanol, water, and acetone, and it was let dry over a hotplate at 100 °C. The substrate was then connected to a potentiostat employing a small metal clamp and the potential scans performed as described in the cyclic voltammetry paragraph in the beginning section of materials and methods. An example of the voltammogram obtained for such device is shown in Figure SI24 (0.1 V/s). It is worth mentioning that the limited stability of the oxidized **AC-P** allows only a limited number of cycles. A real-time video of the experiment described highlighting the color change is provided as Supporting Video S1.

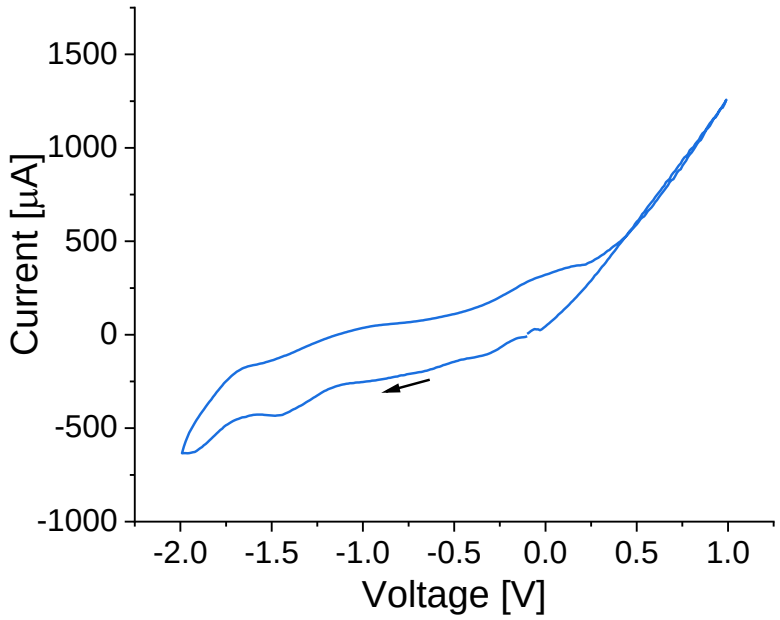

Figure SI24. Example voltammogram scan for the multicolored electrochromic display (0 V → -2 V → 1 V; 0.1 V/s).

IR mapping

5 µL of **AH-P** 15 mg/mL solution in o-dichlorobenzene was drop cast on a BaF_2 substrate for IR transmission analysis. After placing the substrate on a hotplate and heating it up to 100°C, the **AC-P** mouth was prepared employing a cut-up polydimethylsiloxane stamp soaked in a saturated solution of $SnCl_2$ in acetic acid, while the **AQ-P** eyes were obtained from small droplets of a MIBK:TBAF 1M in THF 4:1 solution delivered through a capillary. The sample was then washed with methanol and water, dried, and stored in a desiccator before the measurement. The IR map was measured in transmission mode, and the baseline corrected. The colors of the map shown in Figure 3 of the main text represented the value of the ratio between the absorbance of the band at 3070 cm^{-1} (present in all samples) and that at 1270 cm^{-1}, where different signals are present for the different polymers.

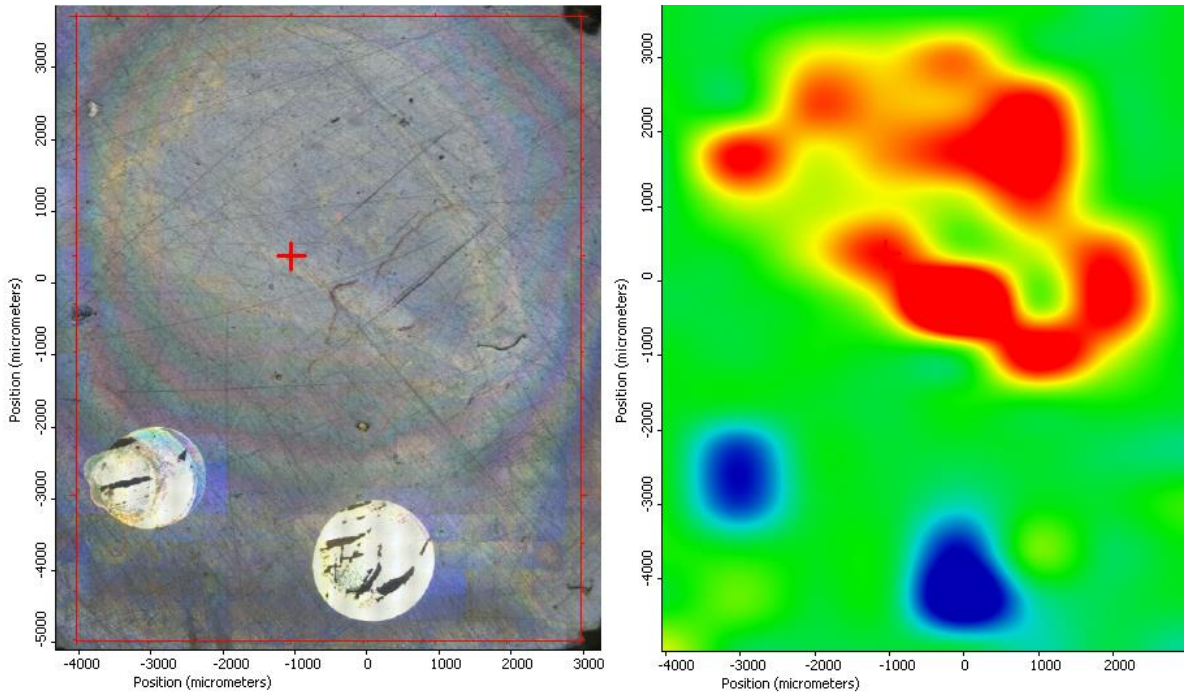

Figure SI25. Left: matrix of optical images taken for referencing the IR mapping. Right: output of the optical IR mapping obtained as described in the text

OFETs fabrication and measurement

A 300 nm thick layer of Parylene N, which will act as dielectric material, was deposited on round-shaped glass substrates, and a 15 mg/mL solution of **AH-P** in ODCB was spun coated on top of them (1000 rpm, 60 s, acceleration 500 ms). **AQ-P** films were prepared by immersion of these films in a 1:4 solution of TBAF 1M in THF:MIBK at 90°C for 3 minutes. **AC-P** films were prepared analogously but employing a solution obtained from 100 mg of $SnCl_2$ and 10 mL of MeOH comprising 1% of HCl 12 M and a temperature of 70 °C. Both these films were then washed thoroughly with MeOH, water, and acetone. The Parylene N was then detached from the glass substrates by slow immersion in water under a 45° angle, so that the polymeric film would float without wrinkling. Pre-patterned Si^{--}/SiO_2 (230 nm) substrates with gold interdigitated source and drain contacts (channel width W = 2 mm, channel length L_C = 20, 10, 5 and 2.5 µm; OFET-Structures Generation 4 design, purchased from Fraunhofer Institute for Photonic Microsystems IPMS, Germany) were cleaned by immersion in boiling acetone (30 min), followed by immersion in isopropanol (5 min, 3 times) and successively plasma treated (oxygen plasma, 60 W for 60 s). Afterwards, they were used to collect from the

top side the active layer previously delaminated in water. The samples were left to dry at 120°C for 5 hours, and an additional Parylene N layer (100 nm) was evaporated on top to fill eventual cracks. To complete the devices, a gate in aluminum was thermally evaporated (PROvap Glovebox Integrated M-Braun Thermal Evaporator). The OFETs based on **AQ-P** films were left in annealing at 120 °C overnight in a controlled nitrogen environment before measuring. Transfer curves of the fabricated transistors were acquired with a semiconductor parameter analyser (Agilent B1500A) inside a glove box with a Wentworth Laboratories probe station.

Field-effect mobility was extracted in both linear (μ_{lin}) and saturation (μ_{sat}) regime from the corresponding transfer characteristic curves according to the Gradual Channel Approximation (GCA), using the two following expressions: $I_{ds} = \mu_{lin} \times C_{diel} \times W/L_C \times [(V_{gs} - V_{TH}) \times V_{ds} - V_{ds}^2/2]$ and $I_{ds} = \mu_{sat} \times C_{diel} \times W/2L_C \times (V_{gs} - V_{TH})^2$, where I_{ds} is the source-drain current, C_{diel} the dielectric capacitance per unit area, W and L_C the channel width and length, respectively, V_{gs} the gate-source voltage, V_{ds} the source-drain voltage and V_{TH} the threshold voltage. The dielectric capacitance C_{diel} can be estimated by knowing the thickness (t_{ins} = 400 nm) and dielectric constant (ε_r = 2.9) of the Parylene layer ($C_{diel} = \varepsilon_r \cdot \varepsilon_0 / t_{ins}$). Then, mobility can be derived from the slope of I_{ds} and $\sqrt{(I_{ds})}$ versus V_{gs} for the linear and saturation regime, respectively, as shown below. Linear mobility was extracted only in the voltage range where the transfer curve is linear, and the saturation mobility where the square root of the transfer curve is linear. Such ranges are highlighted in green in the plots below. They correspond to: V_{gs} from 70 V to 80 V for linear regime, and from 60 V to 80 V for saturation regime in the case of **AQ-P**; V_{gs} from -40 V to -50 V for linear regime, and from -30 V to -50 V for saturation regime in the case of **AC-P** (Figure SI26).

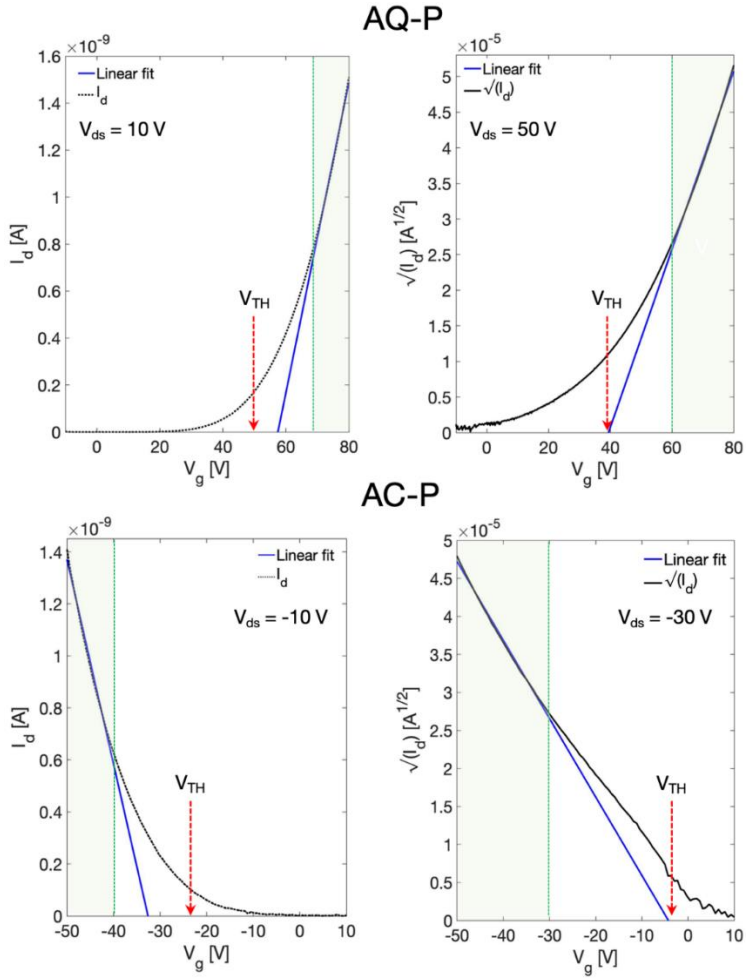

Figure SI26. I_d and $I_d^{1/2}$ vs. V_g plots for the extraction of the mobilities and V_{TH} for **AQ-P** and **AC-P**.

Calculations of the optimized geometries and single-point energies

To evaluate the torsions of the polymer backbone and the energies of the frontier orbitals, we performed DFT calculations on thiophene-terminated model tetramers of the polymers described in this study employing the Orca software package (v5.0.2).[5] For **AC-P** TMS instead of TIPS groups were employed while the triple bonds were left unsubstituted in the case of **AH-P** to facilitate the geometry optimization process. Geometry optimization was performed using B3LYP-D3BJ/def2-SVP basis set and RIJCOSX as an auxiliary basis set as resolution of identity (RI). Remarkably the average torsion angle between the bithiophene units and the **AH**, **AC** and **AQ** units were estimated to be about 15°, 4° and 7° respectively, highlighting the overall higher flexibility and lower degree of aromaticity of **AH-P**.
Single-point energy calculations were performed on the optimized geometries employing B3LYP-D3BJ/def2-TZVP without RI. In both cases, TightSCF was used as convergence criteria. The obtained energy values are summarized in the table below.

	LUMO [eV]	HOMO [eV]
AH-P	-2.12	-5.24
AC-P	-2.74	-4.88
AQ-P	-3.21	-5.65

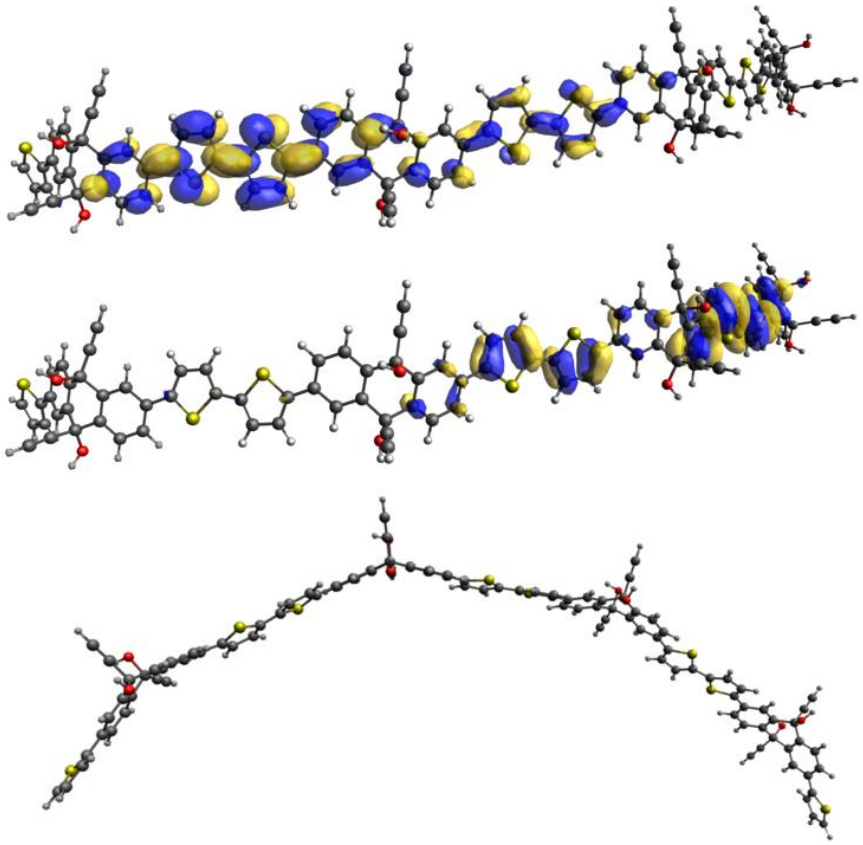

Figure SI27. LUMO (top) and HOMO (middle) isosurfaces for **AH-P** model tetramer. At the bottom, the view from another angle of the optimized geometry.

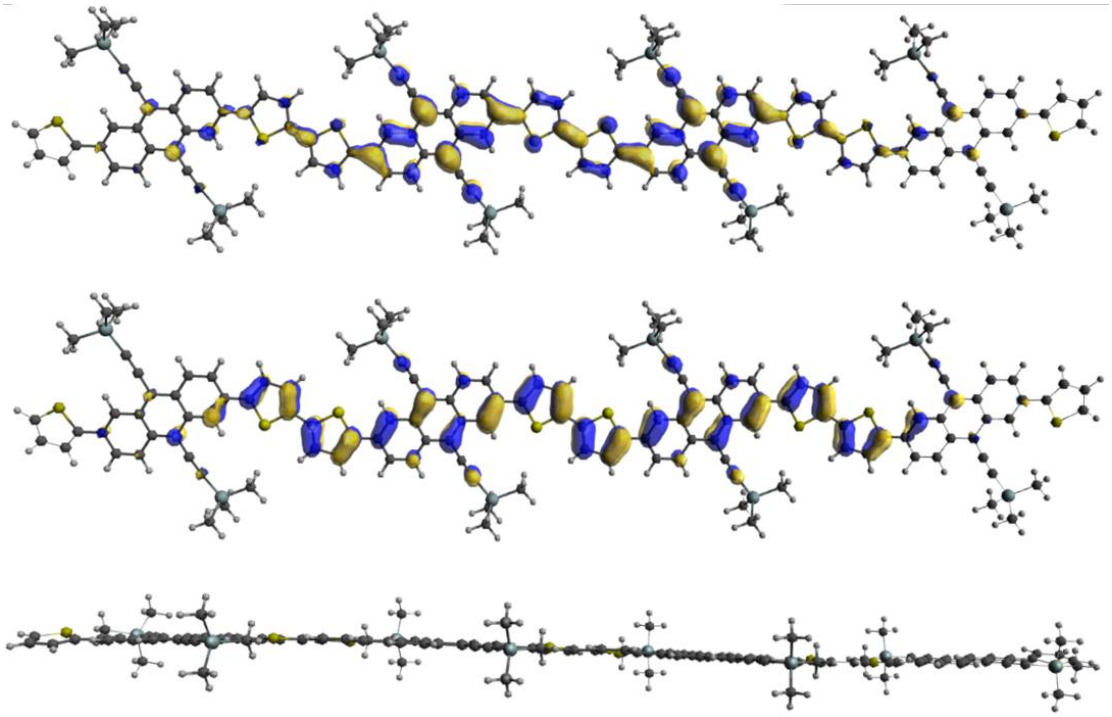

Figure SI28. LUMO (top) and HOMO (middle) isosurfaces for **AC-P** model tetramer. At the bottom, the view from another angle of the optimized geometry.

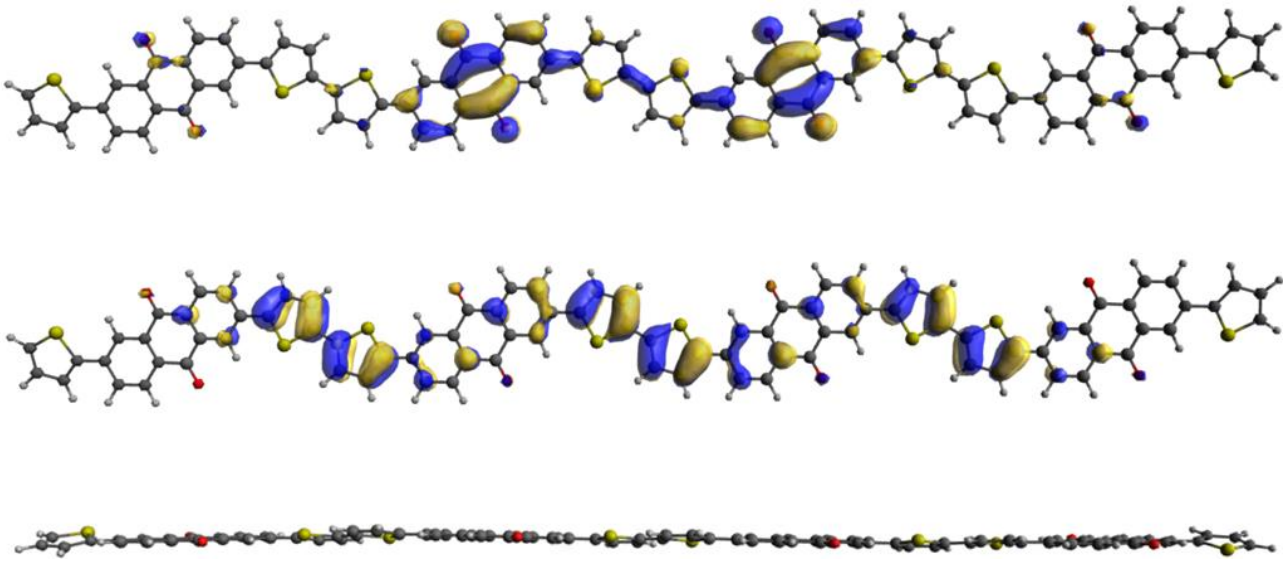

Figure SI29. LUMO (top) and HOMO (middle) isosurfaces for **AQ-P** model tetramer. At the bottom, the view from another angle of the optimized geometry.

DFT Coordinates

AH-P

C	3.02695	1.84744	3.11254
C	3.19376	0.45154	3.07039
C	2.03510	-0.47261	3.46466
C	1.22156	0.18257	4.58647
C	1.05801	1.57680	4.62998
C	1.65986	2.41639	3.50056
C	4.10167	2.66122	2.73997
C	5.31651	2.10763	2.34185
C	5.49646	0.71287	2.30424
C	4.40660	-0.09964	2.67376
C	0.65509	-0.60248	5.59181
C	-0.07430	-0.01958	6.62546
C	-0.24509	1.37448	6.68704
C	0.33712	2.15589	5.67171
C	6.77021	0.10806	1.91447
C	-0.99632	2.01603	7.77172
C	7.16514	-1.21436	2.01387
C	8.48327	-1.45270	1.55325
C	9.11963	-0.31286	1.08924
S	8.05805	1.07006	1.22069
C	-1.58196	3.26729	7.79231
C	-2.23106	3.56917	9.02457
C	-2.13421	2.54851	9.93786
S	-1.24601	1.20795	9.30312
C	1.75516	3.84460	3.86579
O	0.75300	2.27371	2.39635
C	1.17590	-0.72245	2.28948
O	2.56661	-1.72213	3.90631
C	0.48997	-1.00442	1.33225
C	1.80932	5.02610	4.12533
H	3.99035	3.74582	2.78008
H	6.14239	2.77230	2.07794
H	4.49544	-1.18452	2.67095
H	0.80604	-1.68181	5.56706
H	-0.51953	-0.65627	7.39376
H	0.24875	3.24105	5.70872
H	6.52628	-1.99364	2.42907
H	8.96476	-2.43165	1.57021
H	-1.56712	3.94150	6.93529
H	-2.75464	4.50549	9.22394
H	-2.53301	2.50869	10.95045
H	1.21692	2.57337	1.60122
H	2.09758	-2.42191	3.43447
H	-0.12758	-1.23146	0.48370
H	1.85654	6.07315	4.35949
C	10.45451	-0.17290	0.55482
S	11.44114	-1.58193	0.24085
C	11.14327	0.98065	0.21713
H	10.71903	1.97826	0.34138
H	16.45584	3.39520	-2.93434

C	12.77966	-0.60837	-0.32651
C	12.44772	0.73379	-0.27953
C	16.63230	2.33584	-2.92591
H	21.65569	0.70783	-2.51207
C	25.10301	-1.86512	-1.53201
C	24.44831	-2.93679	-0.94707
C	14.02777	-1.22910	-0.77335
H	24.97576	-3.73214	-0.41828
C	20.87791	-0.05650	-2.44495
S	23.94883	-0.77666	-2.26731
C	23.03905	-2.87635	-1.07922
H	19.31309	1.32229	-2.97880
H	14.67465	0.49952	-1.90673
H	13.13958	1.52430	-0.57124
C	16.83113	1.14141	-2.91268
C	19.55502	0.29387	-2.70615
C	14.92406	-0.51203	-1.58825
C	22.59133	-1.75927	-1.76165
H	22.36399	-3.62038	-0.65616
C	14.37743	-2.54077	-0.40368
C	21.21429	-1.36873	-2.06516
H	13.71814	-3.11578	0.25095
C	18.52509	-0.64755	-2.60060
C	16.12448	-1.07230	-2.01879
C	15.57259	-3.10716	-0.83776
C	20.17302	-2.31154	-1.96658
C	17.07257	-0.31604	-2.95245
C	16.45200	-2.38619	-1.64773
C	18.85285	-1.96327	-2.22922
H	15.84807	-4.11485	-0.52643
H	20.38236	-3.33901	-1.67399
O	18.17339	-4.03732	-1.20118
C	17.75741	-3.03015	-2.12370
H	18.08432	-4.89212	-1.64116
O	16.77881	-0.80795	-4.26921
H	17.51231	-0.54765	-4.84503
C	17.55180	-3.65912	-3.44418
C	17.40149	-4.24614	-4.49255
H	17.25968	-4.74454	-5.43306
C	41.47672	0.22025	3.90318
C	26.51963	-1.58541	-1.57984
S	42.66057	-0.68049	4.82229
S	27.68375	-2.80101	-1.10664
C	41.72708	1.57930	3.99970
C	27.16754	-0.42186	-1.96062
H	26.63204	0.47255	-2.28282
H	41.10433	2.33009	3.51070
H	33.01834	2.41586	-3.20802
H	46.00120	6.19222	6.08015
C	43.47154	0.77837	5.34710
C	29.03364	-1.72578	-1.39637
C	28.57875	-0.50328	-1.85789

C	42.84842	1.89023	4.80907
C	33.28888	1.43795	-2.85595
C	46.43224	5.27765	6.44237
H	49.00840	5.44137	11.07605
H	37.70142	1.00928	0.05088
C	40.42697	-0.46503	3.18474
C	50.76619	4.07173	14.87073
C	40.09542	-1.81019	3.20509
C	50.27640	2.79019	14.92835
C	44.63740	0.71613	6.23007
C	30.40997	-2.15629	-1.14614
H	51.28350	4.63212	15.64817
H	40.63199	-2.54092	3.81218
H	50.35121	2.15786	15.81435
C	37.06271	0.12569	-0.01918
C	48.84319	4.45705	10.63177
S	50.47724	4.79632	13.32799
S	39.35584	0.40672	2.11261
C	38.99637	-2.13247	2.37174
C	49.65627	2.38447	13.71143
H	48.07735	5.28197	8.79594
H	35.77156	1.03598	-1.48123
H	45.29433	2.73143	5.78376
H	31.30115	-0.54559	-2.28897
H	43.17579	2.90942	5.01574
H	29.24612	0.32714	-2.08922
C	46.91753	4.24669	6.85225
C	33.59315	0.33528	-2.45855
C	48.31459	4.36953	9.34526
C	35.97803	0.14039	-0.89327
C	31.49080	-1.42108	-1.66923
C	45.48940	1.82902	6.36197
C	49.67378	3.36036	12.73345
C	38.46750	-1.04455	1.70009
H	49.18788	1.41061	13.56605
H	38.60628	-3.14394	2.25936
C	44.93777	-0.43599	6.97987
C	30.70142	-3.29223	-0.36878
C	37.34086	-1.00711	0.76746
C	49.13394	3.29696	11.37123
H	29.88850	-3.87301	0.07347
H	44.28284	-1.30868	6.92322
C	35.14188	-0.97379	-1.02349
C	48.05810	3.12749	8.75416
C	32.81043	-1.79111	-1.42257
C	46.59517	1.80355	7.20864
C	32.01891	-3.67093	-0.12714
C	46.04773	-0.46970	7.81903
C	48.87774	2.05147	10.76855
C	36.49004	-2.12191	0.63562
C	33.98721	-1.02187	-2.02732
C	47.55085	2.99425	7.31541

C	46.88537	0.64054	7.94015
C	33.08165	-2.93038	-0.64753
C	35.41604	-2.11373	-0.24709
C	48.35022	1.96258	9.48433
H	32.23539	-4.53587	0.49994
H	46.25912	-1.35726	8.41559
H	36.63666	-3.00875	1.24969
H	49.08710	1.12603	11.30265
O	47.89026	-0.36918	9.90507
O	34.58733	-4.09327	0.85828
C	34.52525	-3.35645	-0.36313
C	48.10628	0.58277	8.86303
H	34.80762	-5.00711	0.63805
H	48.50254	-1.10221	9.76396
O	34.38603	-1.78319	-3.17756
O	48.65239	2.67557	6.45129
H	35.26453	-1.47180	-3.43957
H	49.38054	3.27093	6.68074
C	35.02122	-4.21850	-1.45515
C	49.29686	0.17270	8.09092
C	35.44032	-4.97866	-2.29943
C	50.27991	-0.21760	7.50141
H	51.14779	-0.54815	6.96241
H	35.80498	-5.63926	-3.06339

AC-P

C	25.05236	0.67530	-0.75470
C	25.71145	-0.55678	-0.41401
C	24.93759	-1.69185	-0.03127
C	23.52324	-1.60998	0.00921
C	22.86487	-0.37848	-0.33271
C	23.63797	0.75855	-0.71091
C	25.86448	1.79003	-1.12958
C	27.23039	1.69861	-1.16785
C	27.90102	0.47427	-0.83681
C	27.12986	-0.61526	-0.47184
C	22.70940	-2.72457	0.38421
C	21.34362	-2.63549	0.41680
C	20.67323	-1.41355	0.07379
C	21.44741	-0.32409	-0.28818
C	29.36170	0.39713	-0.89085
C	19.21687	-1.33207	0.10454
C	30.25525	1.28354	-1.46367
C	31.61632	0.88233	-1.33485
C	31.75531	-0.30546	-0.66056
S	30.22576	-0.94686	-0.17231
C	18.28977	-2.32733	0.36662
C	16.94473	-1.88858	0.29760
C	16.82115	-0.54451	-0.01930

S	18.39743	0.18022	-0.22997
H	25.36764	2.72872	-1.38115
H	27.81885	2.57584	-1.44094
H	27.60562	-1.56554	-0.22647
H	23.20638	-3.65939	0.64875
H	20.97353	0.61982	-0.55923
H	29.94325	2.19080	-1.98138
H	32.45904	1.45218	-1.72913
H	32.67259	-0.83996	-0.41776
H	18.56952	-3.35501	0.59784
H	16.08437	-2.53651	0.47425
C	0.69553	-0.28989	0.05484
S	2.25802	0.48322	-0.07159
C	0.84494	-1.64022	0.33139
C	3.10653	-1.01738	0.24209
C	2.19844	-2.04528	0.43612
H	-0.00299	-2.31654	0.45349
C	4.56472	-1.05738	0.26482
C	5.25779	-2.26453	0.61520
C	5.31944	0.06008	-0.05131
H	4.68753	-3.15739	0.87569
C	6.62603	-2.31262	0.63500
C	6.73814	0.04889	-0.04073
H	4.82790	0.99339	-0.32763
H	2.49812	-3.07276	0.64202
C	7.41953	-1.16826	0.30982
C	7.48999	1.21525	-0.37285
H	7.14077	-3.23655	0.90459
C	8.83545	-1.20693	0.32459
C	8.90627	1.17625	-0.35996
C	9.58692	-0.04153	-0.01104
C	9.70138	2.31889	-0.68822
C	11.00502	-0.05658	-0.00983
S	14.05066	-0.50624	-0.01646
H	9.18773	3.24453	-0.95400
C	11.06999	2.26671	-0.67859
C	11.76155	1.05690	-0.33515
H	11.49490	-0.99184	0.26239
C	13.21945	1.00303	-0.33308
H	11.64134	3.15808	-0.94218
C	15.62181	0.24032	-0.18102
C	14.13919	2.01443	-0.55646
C	15.48859	1.58933	-0.47171
H	13.85134	3.04353	-0.77143
H	16.34471	2.25045	-0.61773
C	-31.56064	-0.13839	0.84205
C	-31.36788	-1.31741	1.51846
S	-30.06355	0.55468	0.32494
H	-32.18276	-1.91490	1.92995
C	-29.99145	-1.66984	1.62448
C	-29.13993	-0.75548	1.03190
C	-27.67856	-0.78127	0.95192

C	-13.93495	-1.93933	0.38302
C	-26.95870	-1.97680	1.28496
H	-13.63014	-2.96717	0.57935
H	-29.63909	-2.56331	2.14025
C	-26.95341	0.33029	0.55968
C	-10.87387	-2.14874	0.53888
C	-15.29071	-1.53712	0.29884
C	-9.50536	-2.18966	0.55986
H	-27.50991	-2.87088	1.58016
C	-25.59145	-2.02029	1.22173
C	-11.57340	-0.94352	0.19448
H	-16.13523	-2.21660	0.42692
C	-13.03195	-0.90820	0.18257
C	-25.53503	0.32141	0.47494
H	-11.43939	-3.04572	0.79552
C	-8.71753	-1.03913	0.24268
C	-24.82667	-0.88256	0.81749
C	-10.82423	0.17815	-0.11982
H	-27.46725	1.25991	0.31223
C	-9.40544	0.17464	-0.10679
H	-8.98616	-3.11194	0.82649
C	-7.30128	-1.06779	0.26714
C	-23.41161	-0.91739	0.74594
C	-24.80900	1.47821	0.06288
H	-25.05685	-2.93751	1.47509
S	-18.21823	-0.18672	0.13450
C	-15.44728	-0.18562	0.03205
C	-8.65953	1.34683	-0.43117
S	-13.88848	0.59232	-0.11019
C	-22.68670	0.24049	0.33686
C	-6.55556	0.10498	-0.05548
C	-23.39364	1.44453	-0.00634
C	-7.24318	1.31842	-0.40626
H	-11.32044	1.10999	-0.39280
C	-21.26988	0.23243	0.26113
C	-16.66487	0.57404	-0.11577
C	-22.62503	2.58049	-0.41229
C	-5.13708	0.10317	-0.03585
C	-20.53967	1.34115	-0.13239
C	-6.45502	2.46935	-0.72149
C	-19.08226	1.30124	-0.19553
C	-21.25764	2.53604	-0.47444
H	-20.75975	-0.69204	0.53322
C	-4.38755	1.22627	-0.34402
C	-5.08645	2.43023	-0.69358
H	-4.64137	-0.82806	0.23997
C	-16.82850	1.91164	-0.44128
H	-6.97400	3.39101	-0.99068
S	-2.07749	-0.30672	-0.00619
C	-18.18593	2.31659	-0.48586
C	-2.92924	1.19297	-0.31477
H	-20.70785	3.42276	-0.79357

H	-4.52046	3.32777	-0.94740
H	-15.98831	2.57869	-0.64239
C	-0.51680	0.47136	-0.12239
C	-2.02348	2.22449	-0.50011
H	-18.49591	3.33495	-0.72021
C	-0.66899	1.82269	-0.39238
H	-2.32545	3.25216	-0.70178
H	0.17751	2.50204	-0.50743
H	-32.50030	0.36263	0.61393
H	-23.15828	3.49520	-0.67691
C	-22.68657	-2.09524	1.07615
C	-21.98600	-3.06449	1.34074
C	-25.52689	2.65660	-0.28017
C	-26.20294	3.63689	-0.56605
C	-6.59559	-2.25298	0.61308
C	-5.91416	-3.22886	0.90214
C	-9.36467	2.53233	-0.77676
C	-10.04510	3.50894	-1.06556
C	9.53580	-2.39547	0.66999
C	10.21482	-3.37369	0.95683
C	6.79064	2.40462	-0.71680
C	6.11467	3.38475	-1.00416
C	25.60269	-2.90034	0.31248
C	26.22331	-3.91544	0.60207
C	22.96163	1.96508	-1.04029
C	22.30209	2.96151	-1.30924
H	20.75805	-3.50727	0.71217
Si	-20.80201	-4.43573	1.69195
C	-21.26390	-5.92430	0.63317
C	-20.89830	-4.87175	3.52235
C	-19.07512	-3.81573	1.25102
Si	-4.75621	-4.60285	1.32370
C	-3.00302	-3.98130	1.00529
C	-5.14466	-6.08751	0.23065
C	-4.97806	-5.04518	3.14168
Si	11.36740	-4.75602	1.36578
C	10.97445	-6.22748	0.25663
C	11.14215	-5.21613	3.17892
C	13.12350	-4.13863	1.05534
Si	27.27087	-5.37381	1.02596
C	26.71788	-6.05252	2.69457
C	29.05582	-4.77395	1.10637
C	27.06412	-6.68096	-0.31558
Si	-27.34564	5.02637	-0.97757
C	-29.10407	4.39754	-0.71979
C	-27.07337	5.52091	-2.77542
C	-26.97982	6.47809	0.16680
Si	-11.19997	4.88584	-1.48557
C	-10.81198	6.36604	-0.38632
C	-12.95444	4.26497	-1.17352
C	-10.97213	5.33371	-3.30147
Si	4.96583	4.76827	-1.41885

C	5.18829	5.21600	-3.23542
C	5.36693	6.24555	-0.32035
C	3.20919	4.15737	-1.09927
Si	21.17579	4.37161	-1.69372
C	21.61199	5.82380	-0.57528
C	19.41096	3.78865	-1.36732
C	21.39173	4.84380	-3.50490
H	27.33218	-6.92167	2.98421
H	25.66478	-6.37560	2.65997
H	26.81291	-5.28779	3.48219
H	27.35763	-6.28463	-1.30091
H	26.01637	-7.01591	-0.38229
H	27.69169	-7.56188	-0.09902
H	13.25788	-3.84260	0.00251
H	13.85823	-4.92781	1.28828
H	13.34881	-3.26159	1.68320
H	10.11125	-5.55203	3.37596
H	11.34877	-4.35318	3.83222
H	11.82804	-6.03250	3.46140
H	22.64800	6.15757	-0.74769
H	21.51749	5.54517	0.48657
H	20.94127	6.67821	-0.76720
H	19.15947	2.92060	-1.99772
H	18.68973	4.59424	-1.58583
H	19.28366	3.48828	-0.31478
H	4.68443	7.08549	-0.53333
H	6.39906	6.59335	-0.48834
H	5.26631	5.98329	0.74509
H	2.97956	3.27699	-1.72092
H	2.47536	4.94671	-1.33444
H	3.07783	3.86813	-0.04413
H	-2.87126	-3.69467	-0.05050
H	-2.26458	-4.76510	1.24459
H	-2.78048	-3.09745	1.62458
H	-6.00742	-5.38320	3.34308
H	-4.77434	-4.17481	3.78600
H	-4.28863	-5.85588	3.43181
H	-19.01702	-3.53530	0.18698
H	-18.32124	-4.59766	1.44370
H	-18.81095	-2.92775	1.84760
H	-21.91105	-5.20975	3.79535
H	-20.65118	-3.99921	4.14828
H	-20.18991	-5.68111	3.76693
H	-29.83991	5.18761	-0.94554
H	-29.25869	4.07115	0.32128
H	-29.31252	3.53641	-1.37495
H	-26.03784	5.86052	-2.93926
H	-27.75190	6.34273	-3.05990
H	-27.26279	4.67072	-3.45030
H	-13.17563	3.38275	-1.79568
H	-13.69188	5.04969	-1.41277
H	-13.08925	3.97563	-0.11887

H	-9.78079	6.71896	-0.54928
H	-10.91680	6.10412	0.67880
H	-11.49767	7.20229	-0.60352
H	29.37059	-4.34319	0.14201
H	29.73916	-5.60415	1.35211
H	29.17247	-3.99354	1.87560
H	21.16110	3.99134	-4.16391
H	22.42735	5.16038	-3.70917
H	20.72009	5.67668	-3.77303
H	4.97783	4.34948	-3.88274
H	6.21976	5.54760	-3.43674
H	4.50422	6.03257	-3.52171
H	9.94310	-6.58007	0.41928
H	11.65942	-7.06631	0.46611
H	11.07732	-5.95787	-0.80676
H	-6.17495	-6.44135	0.39728
H	-4.45727	-6.92195	0.44948
H	-5.04261	-5.82951	-0.83570
H	-11.17525	4.46569	-3.94912
H	-9.94157	5.67062	-3.49862
H	-11.65928	6.14648	-3.59118
H	-25.94477	6.83329	0.03657
H	-27.10966	6.19010	1.22240
H	-27.65960	7.32050	-0.04523
H	-22.27804	-6.28093	0.87568
H	-20.55956	-6.75615	0.80250
H	-21.24130	-5.66799	-0.43822

AQ-P

C	25.08721	0.98227	-0.33884
C	25.75375	-0.22928	-0.06463
C	24.99678	-1.48514	0.22884
C	23.51235	-1.39598	0.21785
C	22.84608	-0.18384	-0.05306
C	23.60322	1.07198	-0.34836
C	25.84741	2.13025	-0.60681
C	27.23487	2.07795	-0.60197
C	27.91825	0.86892	-0.33635
C	27.14867	-0.27637	-0.06850
C	22.75163	-2.54405	0.48615
C	21.36474	-2.49065	0.48795
C	20.68094	-1.28238	0.21498
C	21.45167	-0.13733	-0.05423
C	29.38133	0.82051	-0.34449
C	19.22108	-1.23344	0.21476
C	30.27350	1.75449	-0.84051
C	31.63592	1.37660	-0.68028
C	31.77516	0.15805	-0.06026
S	30.24699	-0.54044	0.33360
C	18.31790	-2.28184	0.28435
C	16.96509	-1.87002	0.26135

C	16.81089	-0.49426	0.17478
S	18.36904	0.29247	0.12318
O	23.02369	2.11987	-0.58674
O	25.57442	-2.53400	0.46740
H	25.31741	3.06253	-0.81007
H	27.80417	2.98928	-0.79220
H	27.61817	-1.24089	0.13489
H	23.28180	-3.47418	0.69853
H	20.79744	-3.39456	0.71528
H	20.98445	0.82341	-0.28009
H	29.95938	2.67891	-1.32578
H	32.47995	1.98161	-1.01428
H	32.69487	-0.36898	0.18991
H	18.62192	-3.32717	0.33700
H	16.12010	-2.55884	0.30474
C	0.61507	-0.38739	0.08921
S	2.17032	0.40628	0.09131
C	0.77282	-1.76303	0.17371
C	3.02642	-1.11608	0.20313
C	2.12597	-2.16886	0.23786
H	-0.06983	-2.45595	0.18609
C	4.48549	-1.15761	0.24969
C	5.16967	-2.37489	0.47942
C	5.25638	0.00470	0.06910
H	4.60350	-3.29458	0.63450
C	6.55609	-2.41968	0.52176
C	6.65020	-0.03344	0.11315
H	4.78993	0.97432	-0.11681
H	2.43172	-3.21318	0.29878
C	7.31669	-1.25444	0.34032
O	6.82666	2.29742	-0.28675
C	7.40636	1.24117	-0.08871
H	7.08572	-3.35716	0.70049
C	8.80002	-1.33538	0.39333
C	8.88972	1.15956	-0.03972
O	9.37934	-2.39086	0.59628
C	9.55627	-0.06186	0.18556
C	9.65054	2.32393	-0.22588
C	10.95023	-0.10161	0.22093
S	14.03409	-0.51195	0.13475
H	9.12090	3.26184	-0.40233
C	11.03723	2.27734	-0.19342
C	11.72137	1.05918	0.03161
H	11.41690	-1.07119	0.40641
C	13.18068	1.01438	0.06212
H	11.60388	3.19558	-0.35535
C	15.59138	0.27759	0.12816
C	14.08336	2.06541	0.03536
C	15.43623	1.65504	0.07336
H	13.77933	3.11144	-0.00044
H	16.28057	2.34594	0.06387
C	-31.77023	-0.15340	-0.09466

C	-31.63906	-1.37558	0.52001
S	-30.23716	0.54684	-0.46544
H	-32.48731	-1.98216	0.84018
C	-30.27885	-1.75503	0.69455
C	-29.38030	-0.81866	0.21482
C	-27.91736	-0.86713	0.22430
C	-14.07726	-2.05221	0.07014
C	-27.23658	-2.07578	0.49842
H	-13.77220	-3.09734	0.12057
H	-29.97131	-2.68273	1.17775
C	-27.14499	0.27834	-0.03436
C	-11.03622	-2.25572	0.35681
C	-15.42990	-1.64435	0.00585
C	-9.64990	-2.30336	0.40022
H	-27.80747	-2.98727	0.68305
C	-25.84925	-2.12766	0.51906
C	-11.71673	-1.04398	0.08990
H	-16.27340	-2.33633	0.00679
C	-13.17566	-1.00024	0.04274
C	-25.75020	0.23185	-0.02168
H	-11.60572	-3.16762	0.54284
C	-8.88602	-1.14601	0.18505
C	-25.08631	-0.97947	0.25972
C	-10.94272	0.11013	-0.12626
H	-27.61216	1.24288	-0.24294
C	-9.54903	0.06954	-0.07920
H	-9.12291	-3.23630	0.60810
O	-6.82699	-2.28011	0.47830
C	-7.40305	-1.22913	0.24470
C	-23.60252	-1.06855	0.28579
C	-24.99063	1.48842	-0.30480
H	-25.32136	-3.05972	0.72874
S	-18.36369	-0.28164	-0.06062
C	-15.58578	-0.26803	-0.07051
C	-8.78903	1.33528	-0.31835
O	-23.02519	-2.11626	0.53030
O	-9.36492	2.38651	-0.55115
O	-25.56612	2.53736	-0.54841
S	-14.02965	0.52395	-0.05776
C	-22.84270	0.18757	-0.00131
C	-6.64302	0.03695	0.00690
C	-23.50660	1.39970	-0.27785
C	-7.30602	1.25243	-0.25779
H	-11.40686	1.07421	-0.34402
C	-21.44841	0.14118	0.01268
C	-16.80514	0.50094	-0.15238
C	-22.74335	2.54839	-0.53615
C	-5.24934	-0.00330	0.05537
C	-20.67493	1.28662	-0.24687
C	-6.54232	2.41005	-0.47142
C	-19.21526	1.23741	-0.23501
C	-21.35667	2.49553	-0.52290

H	-20.98392	-0.82086	0.23874
C	-4.47548	1.15131	-0.15886
C	-5.15608	2.36297	-0.42563
H	-4.78531	-0.96748	0.27298
C	-16.95878	1.87079	-0.30634
H	-7.06939	3.34304	-0.67892
S	-2.16125	-0.41391	0.00663
C	-18.31133	2.28106	-0.35276
C	-3.01651	1.10861	-0.10937
H	-20.78839	3.40170	-0.73804
H	-4.58665	3.27538	-0.60921
H	-16.11348	2.55586	-0.38695
C	-0.60555	0.37946	0.00729
C	-2.11587	2.16106	-0.14536
H	-18.61400	3.32210	-0.46373
C	-0.76290	1.75494	-0.07909
H	-2.42187	3.20533	-0.20604
H	0.08000	2.44756	-0.09159
H	-32.68659	0.37556	-0.35293
H	-23.27138	3.47916	-0.75104

References

[1] M. Nishizawa, T. Ise, H. Koshika, T. Itoh, I. Uchida, *Chem. Mater.* **2000**, *12*, 1367.

[2] B. Dandrade, S. Datta, S. Forrest, P. Djurovich, E. Polikarpov, M. Thompson, *Org. Electron.* **2005**, *6*, 11.

[3] J. H. Park, D. S. Chung, J. W. Park, T. Ahn, H. Kong, Y. K. Jung, J. Lee, M. H. Yi, C. E. Park, S. K. Kwon, H. K. Shim, *Org. Lett.* **2007**, *9*, 2573.

[4] S. S. Birajdar, M. Ourabi, B. Mirka, K. S. More, A. L. Puyad, B. H. Lessard, S. V. Bhosale, S. V. Bhosale, *Chem. – An Asian J.* **2022**, *17*, DOI 10.1002/asia.202200887.

[5] F. Neese, F. Wennmohs, U. Becker, C. Riplinger, *J. Chem. Phys.* **2020**, *152*, 224108.